ANDRÉIA ABADIA BORGES CARNEIRO

Application of Real-time Optimization with Persistent Parameter Adaptation (ROPA) to Processes using Online Parameter Estimation

São Paulo
2020

ANDRÉIA ABADIA BORGES CARNEIRO

Application of Real-time Optimization with Persistent Parameter Adaptation (ROPA) to Processes using Online Parameter Estimation

Thesis submitted to the Polytechnic School of the University of Sao Paulo in partial fulfillment of the requirements for the degree of Masters of Science.

Area of concentration:
Chemical Engineering

Corrected version containing the changes requested by the judging commission on April 14, 2020. The original version is in the collection reserved at the Library of Chemical Engineering (EPQI) and at the Digital Library of Theses and Dissertations of USP (BDTD), according to the Resolution CoPGr 6018, of October 13, 2011.

Supervisor: Prof. Dr. Galo Antonio Carrillo Le Roux

São Paulo
2020

Este exemplar foi revisado e corrigido em relação à versão original, sob responsabilidade única do autor e com a anuência de seu orientador.

São Paulo, _____ de _____ de _____

Assinatura do autor: _____

Assinatura do orientador: _____

Catalogação-na-publicação

Carneiro, Andréia Abadia Borges

Application of Real-time Optimization with Persistent Parameter Adaptation (ROPA) to Processes using Online Parameter Estimation / A. A. B. Carneiro -- versão corr. -- São Paulo, 2020.

79 p.

Dissertação (Mestrado) - Escola Politécnica da Universidade de São Paulo. Departamento de Engenharia Química.

1.Otimização em Tempo Real 2.Dados transientes 3.Filtro de Kalman Estendido 4.Planta dinâmica I.Universidade de São Paulo. Escola Politécnica. Departamento de Engenharia Química II.t.

Acknowledgements

Ser mestre em Engenharia Química sempre fez parte de um grande sonho: minha carreira acadêmica. Obter este título na prestigiosa Escola Politécnica da Universidade de São Paulo, a USP, completa a felicidade deste momento. Não foi fácil chegar até aqui. Tenho muito a agradecer. Primeiramente, a Deus pelo dom da vida. À minha querida e presente mãe por sempre apoiar os meus sonhos e me dar toda a base emocional que preciso nos momentos da vida. Também ao meu pai, Saul Carneiro, pelo apoio e incentivo. Aos meus irmãos, Aida e Saul. Aida, obrigada por sempre acreditar que consigo ir além; é e sempre foi muito importante todo o seu apoio na minha trajetória. Saul, obrigada por estar sempre presente comigo; sei que tenho um grande irmão com quem posso sempre contar. À minha cunhada Gabriele por também ser presente comigo. À minha afilhada, Lívia, e ao meu sobrinho, Saul Neto, por trazerem felicidade nos dias de aflição. Ao meu companheiro, Daniel Valério, por sempre estar presente comigo nos momentos da vida! Também agradeço à sua família, em especial aos seus pais, Daniel e Eliane, pelo amor e apoio.

Ao meu orientador, Galo Antonio Carrillo Le Roux, pela oportunidade de aprendizado e por acreditar no meu trabalho. Obrigada pelos ensinamentos durante o meu mestrado, sem sua ajuda e supervisão eu não conseguiria obter este título. Também agradeço aos meus amigos de caminhada que vivem comigo diariamente trazendo o aconchego de grandes amizades. Aos meus amigos de laboratório e funcionários da USP. E ao Conselho Nacional de Desenvolvimento Científico e Tecnológico (CNPq) pelo apoio financeiro.

"O impossível não é um fato: é uma opinião."

(Mario Sergio Cortella)

Abstract

Recently, there has been an increasing growth in the optimization processes in the industrial area. The reduction of costs, improvement in the quality of final products and minimization of the environmental risks are important issues that companies must take into consideration. Thus, the development of optimization tools to efficiently identify problems has become suitable. In this context, real-time optimization (RTO) methodology is widely used in industrial area to optimize a plant economically. This is a well-established approach to create a link between a regulatory control and the economical optimization of a process under control. There are several RTO methods which can be used in the optimization cycle. The standard RTO method, called Model Parameter Adaptation (MPA), is one of the most applied in industry. Albeit a good method, there are some problems related to the MPA as well as other RTO methods, such as the use of steady-state (SS) data to update SS models to a dynamic plant, the delay in the detection of the SS condition in the system to start the optimization cycle, and the difficulty to model a complete unit since those methods require it. Real-time Optimization with Persistent Adaptation (ROPA) is a new methodology which tackles those issues. ROPA uses transient data to update the model aiming to optimize the plant. Thus, there is no need to wait for the SS condition because the dynamic plant is not updated with stationary information. Aiming to verify the advantages of this new method, this work presents the results of the ROPA application to two chemical processes. All simulations are performed using MATLAB, the dynamic model and the sensitivity equations are solved by SundialsTB. For the first case study, the Williams-Otto reactor, random and deterministic disturbances are considered in the system in order to simulate a real plant. In addition, the Extended Kalman filter (EKF) is used as the online estimator to obtain the estimated parameters and states in the current time. Regarding the Williams-Otto reactor study, the state estimate results show that the filter works consistently, and the state covariance matrix is satisfactorily tuned. Additionally, the parameter estimation shows that ROPA is able to respond to the disturbances occurrence reproducing the actual plant parameter profile. ROPA runs the economic optimization continuously independently of the plant condition. A Monte Carlo analysis of benefits in applying ROPA method in the RTO cycle shows that the method is suitable to track the plant optimum. Regarding the second case study, the Propylene Chlorination process simulated in a commercial dynamic simulator is optimized by an external ROPA implemented in MATLAB. In this case, ROPA can also reach the stationary optimum, and the filter works properly. However, the MPA and ROPA results are similar because the process is in a gas-phase with fast dynamics. Even in this situation, it can be seen that MPA still has the steady-state delay issue.

Keywords: Real-time Optimization (RTO). Transient data. Dynamic plant. Extended Kalman filter (EKF). Online estimation.

Resumo

Recentemente, houve um crescimento crescente nos processos de otimização na área industrial. A redução de custos, a melhoria na qualidade dos produtos finais e a minimização dos riscos ambientais são questões importantes que as empresas devem se preocupar. Assim, o desenvolvimento de ferramentas de otimização tornou-se adequado. Neste contexto, a metodologia de otimização em tempo real (*RTO*) é amplamente utilizada na indústria para otimizar uma planta economicamente. Essa é uma abordagem bem estabelecida para criar um vínculo entre um controle regulatório e a otimização econômica de um processo. O método de *RTO* clássico, também chamado de *Model Parameter Adaptation* (*MPA*), é um dos mais aplicados na indústria. Apesar de ser um bom método, existem alguns problemas relacionados à metodologia *MPA* e aos outros métodos de RTO, como o uso de dados de estado estacionário (EE) para atualizar uma planta dinâmica, a demora na detecção da condição de EE no sistema para iniciar o ciclo de otimização, e a dificuldade de modelar uma unidade completa, uma vez que estes métodos exigem isso. A otimização em tempo real com adaptação persistente (*ROPA*) é uma nova metodologia que aborda esses problemas. O método utiliza dados transientes para atualizar o modelo visando otimizar a planta. Assim, não há necessidade de esperar pela condição de EE, e a planta dinâmica não é atualizada com informações estacionárias. Com o objetivo de verificar as vantagens deste novo método, este trabalho apresenta os resultados da aplicação do *ROPA* em dois processos químicos. Todas as simulações são realizadas no software MATLAB, e o modelo dinâmico e as equações de sensibilidade são resolvidos pelo SundialsTB. No primeiro Estudo de Caso, o reator de Williams-Otto, perturbações randômicas e determinísticas são consideradas no sistema para simular uma planta real. O filtro de Kalman Estendido (*EKF*) é usado como o estimador online para obter os parâmetros e estados estimados no tempo atual. Em relação ao estudo do reator de Williams-Otto, os resultados da estimativa dos estados mostram que o filtro funciona de forma consistente e a matriz de covariância de estado é ajustada satisfatoriamente. Além disso, a estimativa de parâmetros mostra que o método *ROPA* é capaz de responder à ocorrência de distúrbios reproduzindo o perfil real dos parâmetros da planta. O *ROPA* executa a otimização econômica continuamente independentemente da condição da planta. Uma análise Monte Carlo dos benefícios na aplicação do método *ROPA* no ciclo *RTO* mostra que o método é adequado para obter o ótimo da planta. No segundo Estudo de Caso, o processo é simulado em um simulador dinâmico comercial e é otimizado por um *ROPA* externo implementado no MATLAB. O *ROPA* também pode atingir o ótimo estacionário da planta e o filtro funciona corretamente. No entanto, os resultados *MPA* e *ROPA* são semelhantes porque o processo está na fase gasosa com uma dinâmica rápida. Mesmo nesta situação, pode-se ver que o *MPA* ainda lida com o problema de atraso no estado estacionário.

Palavras-chave: Otimização em Tempo Real (RTO). Dados transientes. Planta dinâmica. Filtro de Kalman Estendido. Estimativa em linha.

List of Figures

List of Tables

List of abbreviations and acronyms

ARX	Auto-regressive model with exogenous inputs
CSTR	Continuous stirred-tank reactor
DRTO	Dynamic real-time optimization
EKF	Extended Kalman filter
EMPC	Economic model predictive control
FCC	Fluid Catalytic Cracking
HRTO	Hybrid real-time optimization
ISOPE	Integrated system optimization
MPA	Model parameter adaptation
MPC	Model predictive control
QP	Quadratic programming
ROPA	Real-time Optimization with Persistent Parameter Adaptation
RTO	Real-time optimization
SCFO	Sufficient conditions for feasibility and optimality
SQP	Sequential quadratic programming
SS	Steady-state
UKF	Unscented Kalman filter

List of symbols

General notation

$\hat{x}_k$ estimated states

$\hat{\theta}_k$ estimated parameters

y^{sp} optimal values

y_p plant input-output mapping

u system inputs ($\boldsymbol{u}_k \in \mathbb{R}^{n_u}$)

d_p deterministic disturbances ($\boldsymbol{d}_p \in \mathbb{R}^{n_d}$)

ε_p random disturbances ($\boldsymbol{\varepsilon}_p \in \mathbb{R}^{n_n}$)

k time k

f_{ss} steady-state model

x system states (n_x)

p system parameters (n_p)

y system outputs (n_y)

h output function

v_{ss} measurement noise - Gaussian random noise with zero mean and constant covariance matrix $\boldsymbol{R}_p$

f_{dyn} dynamic discrete model

w_k process noise – Gaussian random noise with zero mean and constant covariance matrix $\boldsymbol{Q}$

v_k measurement noise – Gaussian random noise with zero mean and constant covariance matrix $\boldsymbol{R}$

z process measurement used in steady-state detection

z_f filtered value of the measurement used in steady-state detection

λ_1 filter factor for z_f

$\delta_{1,f}$ variance of the measurement z with its filtered tendency z_f

λ_2 filter factor for $\delta_{1,f}$

$\delta_{2,f}$ variance between two consecutive measurements z

λ_3 filter factor for $\delta_{2,f}$

R_{SS} ratio of variances

p^{adj} adjustable parameter set

p^{nom} non-adjustable parameter set

Φ_{adap} objective function of the model adaptation problem

R_p weights used in Φ_{adap}

G_{adap} constraints of the model adaptation problem

$p^{L,adj}$ adjustable parameter set lower bounds

$p^{U,adj}$ adjustable parameter set upper bounds

g_i inequality constraints

h_i equality constraints

$\bar{x}$ optimum point for a general optimization

α updates of measurement adjustments in a general economic optimization

β updates of parameters in a general economic optimization

Δt_{ROPA} period between two consecutive ROPA executions

$p^{adj,\star}$ adjustable parameters in the solution of the optimization problem

x^e extended system states

w^p parameter noise – Gaussian random noise with zero mean and constant covariance matrix Q^p

f^e extended dynamic model

h^e extended output function

w^e extended noise array

$\hat{x}^e$ estimated extended states

F linearized extended dynamic model

H linearized extended output model

P estimate covariance matrix

K filter gain

G constraints of the steady-state economic optimization

$\mathcal{U}$ operational contraints

u^L inputs lower bounds

u^U inputs upper bounds

y^L outputs lower bounds

y^U outputs upper bounds

Φ_{profit} economic objective function

Chapter 4: Case Study 1 - Williams-Otto rector

F_R reactor outlet mass flow rate [kg/s]

F_A reactor inlet mass flow rate of component A [kg/s]

F_B reactor inlet mass flow rate of component B [kg/s]

X_A mass fraction of component A [-]

X_B mass fraction of component B [-]

X_C mass fraction of component C [-]

X_E mass fraction of component E [-]

X_P mass fraction of component P [-]

X_G mass fraction of component G [-]

t time [s]

M_t mass holdup [kg]

k_i reaction rate constant of the i^{th} reaction [1/s]

A_i frequency factor of the i^{th} reaction [1/s]

E_i activation energy of the i^{th} reaction [K]

T_R reactor temperature [ºC]

T_R reference temperature for parameter rearrangement [K]

Φ_i rearranged parameters of the i^{th} reaction [-]

Ψ_i rearranged parameters of the i^{th} reaction [-]

Chapter 5: Case Study 2 - Propylene Chlorination process

r_j reaction rate of the j^{th} reaction

k_i reaction rate constant of the j^{th} reaction [lbmol/h ft³ atm²]

$p_j{}^*$ partial pressure of propylene for reactions (1) and (2) and of allyl chloride for reaction (3) [atm]

p_{Cl_2} partial pressure of chlorine [atm]

A_j kinetic coefficient of j^{th} reaction [lbmol/h ft³ atm²]

B_j kinetic coefficient of j^{th} reaction [-]

V reactor volume [ft³]

P reactor pressure [atm]

T reactor temperature [ºR]

N_i number of moles of component i [lbmol]

R ideal gas constant [BTU/lbmol ºR]

C_p heat capacity of reaction mixture at constant pressure [BTU/lbmol ºR]

C_v heat capacity of reaction mixture at constant volume [BTU/lbmol ºR]

Δh_1 heat of the reaction (1) [BTU/lbmol]

Δh_2 heat of the reaction (2) [BTU/lbmol]

Δh_3 heat of the reaction (3) [BTU/lbmol]

F_{in} inlet molar flow rate of component i [lbmol/h]

F_{out} outlet molar flow rate of component i [lbmol/h]

T_{in} reactor inlet temperature [ºR]

$\dot{Q}$ heat flow [BTU/lbmol]

Contents

1 INTRODUCTION AND LITERATURE REVIEW

This Chapter discusses the real-time optimization (RTO) applied to processes, and it describes some RTO methods emphasizing the standard method (Model Parameter Adaptation – MPA) which is the most used method in industrial applications. Moreover, the common issues and challenges associated with this methodology are presented, and other kinds of methods which tackle the RTO problems are shown. The Real-time Optimization with Persistent Adaptation (ROPA) method is cited as a new option to get better solutions in the optimization cycle.

1.1 Real-time optimization – RTO

More recently, there has been an increasing pressure to improve the quality in the final products, reduce costs and minimize the environmental risks in the industrial area, hence the development of optimization tools to efficiently identify problems has become suitable. Many factors have contributed to develop these optimization tools. The high technology in the computer area and the power of computers have allowed the application of mathematical models. Moreover, improved models have been developed to represent chemical plants, and recently software for optimization has provided new and better ways to solve problems (GROSSMANN and BIEGLER, 1995).

In general, process optimization can be understood as a procedure involving five main steps: updating model parameters; determining process constraints; thermodynamics, equilibrium and kinetic relationships (the process models); feed and product values, and the control system. The success of the optimization process depends on the relative accuracy of these respective steps, and its improvements will enhance the process operation. Otherwise, inaccuracy in even one of these tasks can decrease the profitability of plant operation (CUTLER; PERRY, 1983).

A well-established approach to create a link between a regulatory control and a business optimization of a process under control is called real-time optimization - RTO (ENGELL, 2007). The RTO methodology was made possible for the first time in the mid to late 1980s, due to several developments, such as: model predictive control technology; open equation modeling, computer processing capability (speed,

memory, affordable cost), and large scale, and sparse matrix SQP solvers. This methodology uses a rigorous steady-state model of the process which implies the use of multi-component mass and energy balances, vapor-liquid equilibrium expressions, and reaction kinetics. However, other expressions that are not easily modeled can be required to describe some effects in the process (DARBY et al., 2011). There are many applications of real-time optimization in the literature, as: in a high-purity distillation column (DIEHL et al., 2002), in a SO_2 conversion process (JIA et al., 2017), in a fluid catalytic cracking unit (MATIAS and LE ROUX, 2018), in a fed-batch reactor for penicillin production (AHMAD; GAO; ENGELL, 2018) and in a reactor (PAPASAVVAS et al., 2019).

Several methods can be used in the RTO methodology. Some of them are shown and studied in Graciano (2015): the Integrated System Optimization and Parameter Estimation (ISOPE), the Modifier Adaptation and the Simple Central Force Optimization (SCFO) methods. Each method tries to solve the economic-based optimization problem using different assumptions. For instance, the ISOPE method handles the structural plant-model mismatch adding a term in the objective function coming from the parameter estimation step. All of these RTO algorithms have been developed in the literature, and they aim to converge to the real optimum point.

The Model Parameter Adaptation (MPA) method is the most used method in industry. There are three main steps in the MPA optimization cycle: steady-state detection, model adaptation and steady-state optimization. The SS detection is a difficult task when handling with dynamic plants. The plant data need to pass through a statistical algorithm in which the SS condition is established when all of the algorithm requirements are respected. Since a dynamic system is subjected to disturbances, the SS operating point is not stable. Moreover, when there are disturbances in the process, the optimization algorithm needs to wait until the new SS point is settled to run the optimization cycle again. These issues are discussed in the following Section.

1.2 Problems related to the RTO methodology

There is a general hierarchy for control and decision making in a plant operation. The main steps of this process are: planning, scheduling, optimization,

advanced control and regulatory control (ZANIN, 2001), as shown in Figure 1. The integration of these steps can be a problem in the process of control and optimization in a plant. The generated information in each layer needs to be accurately used in the next steps. The coordination between the tasks can avoid conflict and inconsistency (MATIAS and LE ROUX, 2018).

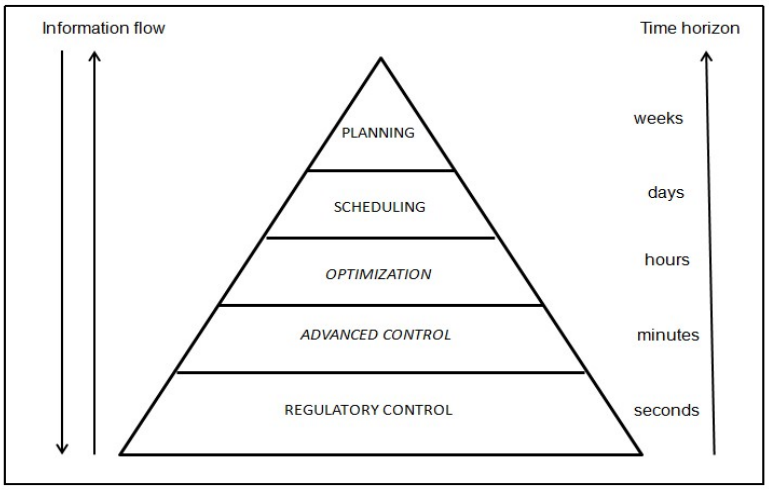

Figure 1 - Plant hierarchy (Source: Adapted from ZANIN, 2001).

Updating a steady-state model to a dynamic plant is another concern in the RTO methods. In most of the applications, steady-state models are used for online process monitoring, product property prediction, online optimization, etc. In an online optimization, the plant data are used to tune these models from time to time to be able to represent the dynamic process using the static model. The starting step to optimize a plant using a RTO method is the steady-state identification, and a total disorder in the optimization process can appear if the real steady-state is not correctly detected (BHAT; SARAF, 2004). The steady-state periods detection depends on the process and on the disturbances that affect the process operation, and there are cases in which steady-state points are nonexistent. The more complex the process, the more challenging it is to detect if the plant has reached steady-state. It is important to use right SS values to have a precise optimization process (MATIAS and LE ROUX, 2018).

The steady-state wait is another problem in the RTO methods. After the steady-state point is well-established in a given time, the model will be updated, and the new optimal values will be sent to the plant. However, there is a specific time in the implementation of the RTO algorithm in each optimization cycle, and there is no guarantee that the previously updated model is still in phase with the current plant

operation. It may due to some new disturbances affecting the process. Moreover, the steady-state detection takes a long time because complex criteria may need to be checked to determine that the unit has reached steady-state (FRIEDMAN, 1995).

Modeling of the complete unit is practically impossible, so it is more common to have the optimization of a single unit in industrial applications. The local optimizers cover only a local subset of the problem. Although the solution for this problem cannot encompass the whole process, this is a way to try to optimize the plant since some units will never have good complete models (FRIEDMAN, 1995). It is possible to have a single RTO implementation to a specific section of the plant when dealing with steady-state optimization, but it is necessary to specify the prices and composition of the intermediary streams which is a challenge to the optimization process (MATIAS and LE ROUX, 2018).

1.3 Trying to tackle RTO problems

As discussed previously, the standard RTO method (MPA) starts with the steady-state detection module which decides if the plant has reached steady-state, based on statistical criteria. Afterwards, the SS point goes through the parameter estimation block to update the model (GRACIANO, 2015). Thus, the problem related to the steady-state wait is an issue in this case. Also, as mentioned before, it is not possible to have the optimization of an isolated unit when using traditional RTO methods (FRIEDMAN, 1995). Hereby, there are some RTO methods in the literature which bring solutions to avoid these problems.

Recently, in addition to the static optimization, there have been developments in the use of Dynamic RTO (DRTO) which use a dynamic model instead of SS model. Although this type of method may eliminate requirements of the steady-state detection in the optimization cycle, the solution for large-scale nonlinear dynamic systems is a challenge for RTO implementations, even with the power technology in computer area. To try to address the computational challenges, a “Hybrid RTO” (HRTO) which uses a dynamic model in the model adaptation layer and SS model in the business optimization step can also be considered (KRISHNAMOORTHYA; FOSS; SKOGESTAD, 2018). Figure 2 shows a general scheme of the HRTO.

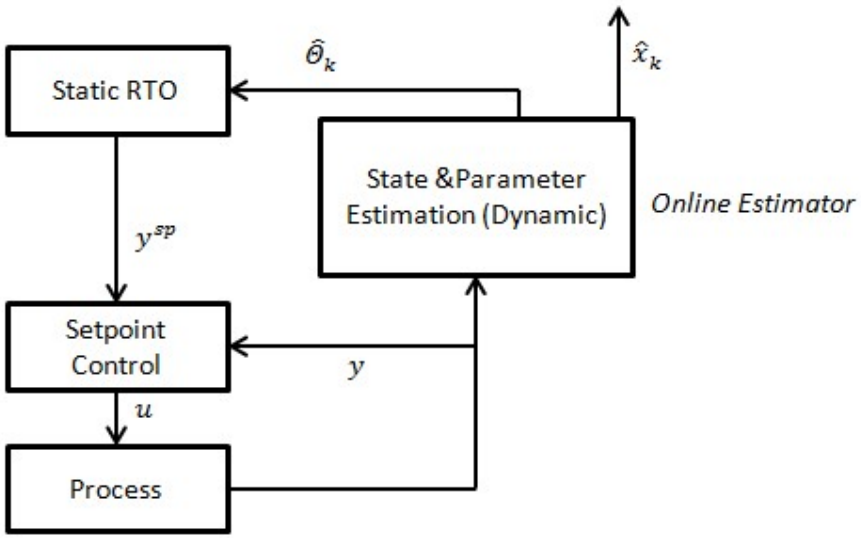

Figure 2 - General HRTO scheme (Source: KRISHNAMOORTHYA; FOSS; SKOGESTAD, 2018).

In a general HRTO implementation, the process data is sent to the state and parameter estimator step which uses a dynamic model (transient data) to obtain the states $(\hat{x}_k)$ and the estimated parameters $(\hat{\theta}_k)$. These set of parameters are used in the static economical optimization which generates the optimum of the plant (y^{sp}) that optimizes the objective function in the current time.

Real-time Optimization with Persistent Adaptation (ROPA) method is a new methodology in the optimization area, and it brings a different way to treat the problem. The method aims at tackling the problems associated with classical RTO methods and getting better solutions for the problem. ROPA is described and compared to MPA method in Chapter 2.

1.4 Motivation and objectives

Recently, there has been an increasing competition amongst industries, and the interest in the economic optimization of processes has becoming more crucial. In this context, the study and development of real-time optimization (RTO) tools overlap this interest. Commonly, RTO methodology uses nonlinear steady-state process models to compute the optimal setpoints in order to optimize the process. It can be due to two reasons: the economic operation process is often done at the steady-state condition, and the control inputs are provided as setpoints and are kept constant for a long period of time what makes the implementation easier. Moreover, constraints, such as process and equipment constraints, storage and capacity constraints and

product quality constraints are also considered in the RTO cycle (KRISHNAMOORTHYA; FOSS; SKOGESTAD, 2018). However, this classical RTO methodology faces some challenges, as mentioned in Section 1.2, such as the steady-state wait and the update of a steady-state model to a dynamic plant.

Different RTO approaches have been developed to reach a more profitable process, and they aim at tackling the standard RTO issues. The Dynamic RTO (DRTO) and Hybrid RTO (HRTO) methods which were previously mentioned in Section 1.3 are examples of these approaches. In addition, Real-time Optimization with Persistent Adaptation (ROPA) is also a method that handles with the RTO challenges aiming to have more efficient optimization processes. According to Darby et al. (2011), a fundamental limiting factor of the RTO methodology is the steady-state wait since the optimization process occurs at lower frequencies because the process needs to be at the SS condition. Once most of the processes are subjected to disturbances, they are often at a non-steady state condition, so the classical RTO algorithm needs to wait for the next SS point to start the calculations what spends more time in the optimization process. ROPA brings an alternative for this issue since it does not require the SS condition to start the optimization cycle. Hence, the increase of the optimization process frequency enhances the prediction and disturbances detection capacity.

There have been many studies in the RTO area with the objective of improving the RTO method algorithm in which aims to converge to the plant true optimum even with uncertainties due to disturbances. The RTO application to processes can provide important information to better understand the process and the best way the process needs to be modulated in order to reach a more profitable operation.

Given the advantages of the ROPA method, the main contribution of this project is the application of ROPA method to processes aiming to obtain better solutions in the optimization cycle. The results of these applications can provide evidences that ROPA converges to the actual plant optimum even using transient data in a steady-state optimization. Due to the use of dynamic information, the SS wait issue is not a problem anymore, and the SS detection layer is not necessary in the optimization cycle, as in the standard RTO method. Two case studies are used to identify these ROPA benefits: the Williams-Otto reactor and the Propylene Chlorination process. In the first case study, the ROPA implementation in the Williams-Otto reactor, the main objective is to reproduce the ROPA and MPA

algorithms in MATLAB and show that ROPA can reach the plant stationary optimum even subjected to disturbances. The results also show that the Extended Kalman filter works properly. Moreover, in the first case study, Monte Carlo analyses are used to obtain more information about the economic performance of both methods in different scenarios. Regarding the second case study, the software Aspen Plus Dynamics is used to simulate the process. The propylene chlorination process is considered as the plant. The main contribution of this second case study is that the process simulated in a commercial dynamic simulator is optimized by an external MPA and ROPA implemented in MATLAB what represents a more realistic RTO implementation. In this case, ROPA also reaches the stationary optimum even under disturbances, and the filter also works correctly with its tuning parameters in the second case study. However, ROPA and MPA results are similar since the case study is a gas-phase process with fast dynamics. Therefore, the ROPA benefits cannot be seen as when the method is applied to a process with low dynamics, as in liquid phases.

1.5 Thesis overview

The thesis is organized as follows. First, in Chapter 2, Model Parameter Adaptation (MPA) and Real-time Optimization with Persistent Adaptation (ROPA) methods are described and compared. In Chapter 3, mathematical preliminaries are described in order to explain how MPA and ROPA methods work. Chapter 4 focus on the Williams-Otto reactor study which applies the MPA and ROPA methods to compare them. Chapter 5 presents the MPA and ROPA implementations in the Propylene Chlorination process. Finally, Chapter 6 concludes the thesis and proposes future work recommendations.

1.6 Publication associated with this project

- **2019 - Process Systems Engineering (PSE) – Rio de Janeiro/Brazil.** CARNEIRO A.A.B. and Le ROUX G.A.C. Poster Session: *Application of Real-time Optimization with Persistent Parameter Adaptation (ROPA) to a Continuous Stirred Tank reactor (CSTR)*

2 MODEL PARAMETER ADAPTATION (MPA) AND REAL-TIME OPTIMIZATION WITH PERSISTENT ADAPTATION (ROPA) METHODS

This Chapter *presents the classical and the new RTO methods which are called Model Parameter Adaptation (MPA) and Real-time Optimization* with *Persistent Adaptation (ROPA)*, respectively. It also compares them in order to show the main differences between both of the methods.

2.1 Model Parameter Adaptation (MPA): the standard RTO method

The RTO methodology is one of the most applied optimization in industry (DARBY et al., 2011). The classical RTO method which is called Model Parameter Adaptation (MPA) assumes that model and disturbance transients are neglected if the optimization sampling time is long enough that the process can be indicated as a process at the steady-state point (ADETOLA; GUAY, 2010). The three main steps of this method are steady-state detection, parameter estimation, and economic optimization, and these steps are shown in Figure 3 below.

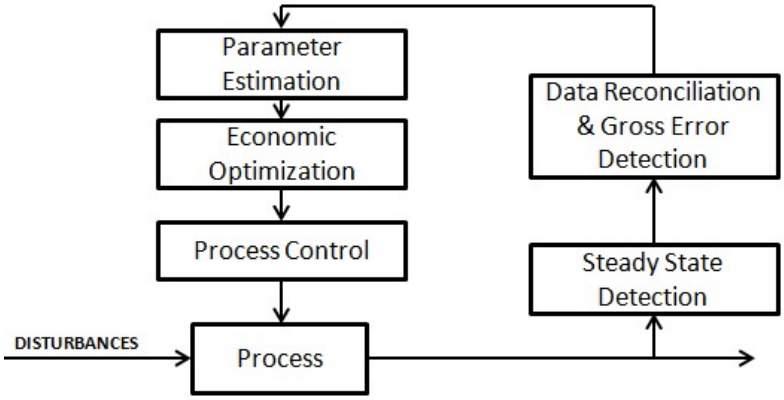

Figure 3 - Classical RTO - Model Parameter Adaptation – (MPA) scheme (Source: GRACIANO, 2015).

The first task is to analyze the plant data to detect if the process is (reasonably) steady. Subsequently, in some cases, the stationary point can go through the data reconciliation and gross error detection stage. In the parameter estimation step, the steady-state data are used to update some key parameters of the model such that it can represent the plant in the actual condition. The third step uses the fitted (adjusted) model to find a new optimal operation point which becomes the new set point for the control system (MENDOZA et al., 2013).

The detection of the steady-state (SS) is an important step, and it needs to be carefully done. Real-time optimization uses a rigorous steady-state model, so the process data need to be collected when the process reaches the SS condition. Otherwise, erroneous parameters will be used, and the aiming to optimize the system can fail. Furthermore, the application of the steady-state model to the real plant should be implemented with the right parameter values to guarantee meaningful results. Different methods have been developed to detect the steady-state points. For instance, Jiang et al. (2003) present a method based on wavelet transform that can be used in continuous processes, and an application of this method was done to crude oil unit and pulp mill recausticizing plant. Also, Rincón, Le Roux and Lima (2015) show an approach for steady-state identification which is a method based on the auto-regressive model with exogenous inputs (ARX), and they compare this method to other three methods: F-like test, wavelet transform and a polynomial-based approach. The method which will be used to detect the steady-state point in a RTO implementation will be chosen according to the process characteristics.

After the steady-state condition is established, the first optimization layer in the classical RTO methodology (the parameter estimation) is done. This step uses the plant information, and the best values of parameters that represent the current operating point are found. The economic optimization step, the second optimization layer, uses the updated rigorous steady-state model to optimize the plant economically. It is more common to have the profit or the cost of the operation as the business function (QUELHAS; JESUS; PINTO, 2013).

Between the steady-state detection and the parameter estimation layers there is the data reconciliation and gross error detection block. In this step, the process data are submitted to gross error detection aiming to remove errors from instrument malfunction. Afterwards, the reconciliation is done to correct the model inputs and outputs and to adjust the measurements, satisfying the material and/or energy balances. The data reconciliation is formulated as an optimization problem which minimizes the difference between measured variables and the estimated model variables (SCHLADT; HU, 2007).

2.2 Real-time Optimization with Persistent Adaptation (ROPA)

The Real-time Optimization with Persistent Adaptation (ROPA) method was developed by Matias and Le Roux (2018) to tackle some problems related to the standard RTO methodology. The method integrates online parameter estimation in the optimization cycle using transient data via online estimators. Hence, ROPA avoids the inherent steady-state wait and the use of SS data in a dynamic plant. After the parameter estimation is done, the parameter values are used to calculate the economic optimum set points for the plant as in the other RTO methods. ROPA brings an intermediary solution between static and dynamic optimization, and it is also a possible key for decoupling the estimation problem aiming to optimize the entire plant.

In Matias and Le Roux (2018), ROPA was applied to three simulation case studies: the Williams-Otto reactor, a Fluid Catalytic Cracking unit (FCC) and a process composed of two stages. In the Williams-Otto plant and the FCC unit, the objective was to show that when online estimators using transient data are used to update the steady-state model in a continuous optimization, the computed solution tends to the SS optimum. Thus, the problem related to the SS wait could be avoided when using ROPA method. In both cases, ROPA was compared to MPA method, and there were benefits of using ROPA method in the optimization cycle. In the third case study, ROPA was applied in a process composed of two stages represented by a distillation column and a reactor. The aim was to show that ROPA can decouple the estimation problem to obtain the plant-wide optimum. The results of this case showed that ROPA is able to drive the complete system to the optimal plant-wide steady-state.

2.3 Comparison between MPA and ROPA methods

As mentioned before, MPA is the standard RTO approach, and it deals with the steady-state wait problem. The detection of a SS point is a difficult task in the optimization of a plant. Many commercial RTO software use either statistical or heuristic methods or both to verify if the plant has reached the stationary point. The detection of SS is determined regarding a tolerance specified by the user, and it is detected when all the measurements are within this value. If the tolerance is not

specified within proper evaluation, transient data might be used erroneously in the SS model. Clearly, if transient data has been used in static models, there may be estimation errors in the optimization cycle (KRISHNAMOORTHYA; FOSS; SKOGESTAD, 2018).

The main difference between MPA and the new method ROPA is the use of different types of models in the parameter estimation layer. MPA uses a steady-state model, and ROPA uses a dynamic model. Figure 4 compares MPA to ROPA.

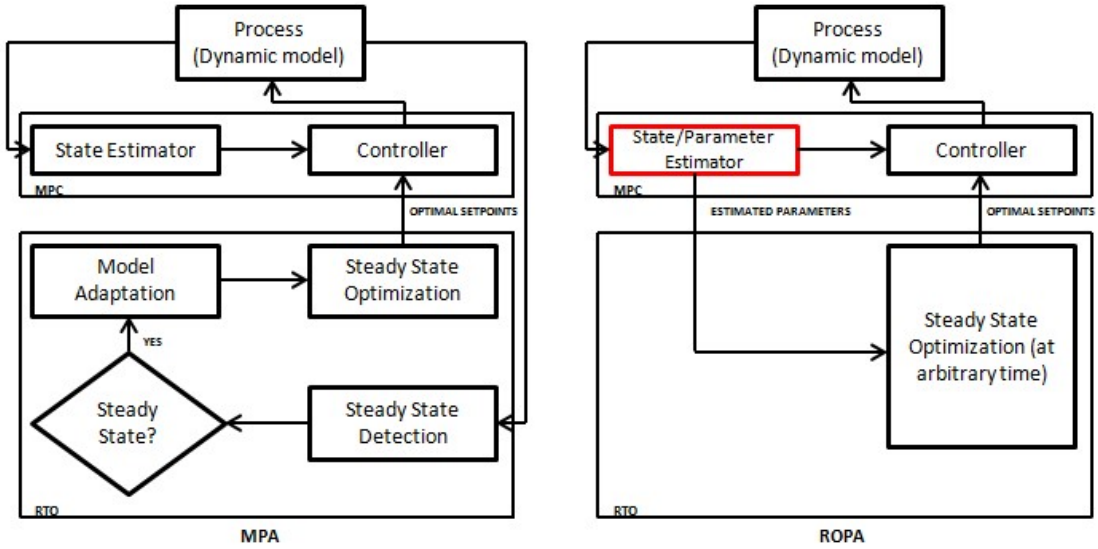

Figure 4 - Comparison between MPA and ROPA methods (Source: MATIAS and LE ROUX, 2018).

A valuable advantage of ROPA method is that the detection of the steady-state is not necessary since the approach uses transient data to update the model in the current point. Online estimators are used to estimate the parameters in the optimization cycle, such as extended Kalman filter and reduced extended Kalman filter. The online estimator is chosen depending on the model characteristics, and it estimates the states and the parameters at each sample time.

3 MATHEMATICAL FUNDAMENTALS FOR REAL-TIME OPTIMIZATION

This Chapter introduces the mathematical preliminaries to solve an optimization problem using real-time optimization methods. First, the introduction of useful information about the process (used models and notation) is given. Secondly, a general nonlinear optimization problem is shown and explained. Lastly, the MPA and ROPA methodologies are detailed mathematically.

3.1 The process

The equations and notation for each studied process is based on Matias and Le Roux (2018). The plant is represented by the following steady-state (SS) input-output mapping:

$$\boldsymbol{y}_{p,k}\left(\boldsymbol{u}_k, \boldsymbol{d}_{p,k}, \boldsymbol{\varepsilon}_{p,k}\right) \in \mathbb{R}^{n_y} \tag{1}$$

in which $\boldsymbol{u}_k \in \mathbb{R}^{n_u}$ are the system inputs, $\boldsymbol{d}_{p,k} \in \mathbb{R}^{n_d}$ are the deterministic disturbances, and $\boldsymbol{\varepsilon}_{p,k} \in \mathbb{R}^{n_n}$ the random disturbances. The subscript k indicates the variable at time $\boldsymbol{t}_k$ assuming a zero-order holder over the interval $[t_k, t_{k+1})$.

The steady-state model is represented by (2) and (3):

$$\mathbf{0} = \boldsymbol{f}_{ss}(\boldsymbol{x}, \boldsymbol{u}, \boldsymbol{p}) \tag{2}$$

$$\boldsymbol{y} = \boldsymbol{h}(\boldsymbol{x}, \boldsymbol{p}) + \boldsymbol{v}_{ss} \tag{3}$$

where $\boldsymbol{x} \in \mathbb{R}^{n_x}$ are the model state variables and $\boldsymbol{p} \in \mathbb{R}^{n_p}$ is the set of parameters. The subscript ss is associated with SS, and the lack of time subscript indicates steady-state values. The steady-state function $\boldsymbol{f}_{ss}$ is nonlinear.

The dynamic model, with subscript dyn, is represented by (4) and (5):

$$\boldsymbol{x}_{k+1} = \boldsymbol{f}_{dyn}(\boldsymbol{x}_k, \boldsymbol{u}_k, \boldsymbol{p}_k) + \boldsymbol{w}_k \tag{4}$$

$$\boldsymbol{y}_k = \boldsymbol{h}(\boldsymbol{x}_k, \boldsymbol{u}_k) + \boldsymbol{v}_k \tag{5}$$

where $\boldsymbol{w}_k$ and $\boldsymbol{v}_k$ are the process and measurement noises. Both are modeled as white-Gaussian random noises with zero mean and constant covariance matrices $\boldsymbol{Q} \in \mathbb{R}^{n_x, n_x}$ and $\boldsymbol{R} \in \mathbb{R}^{n_y, n_y}$, respectively. The state transition function $\boldsymbol{f}_{dyn}(\boldsymbol{x}_k, \boldsymbol{u}_k, \boldsymbol{p}_k)$ is also a mapping over the interval $[t_k, t_{k+1})$, and it represents the solution of the differential model during the period. $\boldsymbol{f}_{dyn}$ is assumed to be at least once differentiable in all points in the studied range, and it has the same dimension and states as $\boldsymbol{f}_{ss}$.

3.2 General nonlinear optimization problem

A general nonlinear optimization problem can be represented by the following problem (6) considered in Bazaraa; Sherali; Shetty, 2006:

$$min\ \boldsymbol{f}(\boldsymbol{x})$$

$$s.t. \begin{cases} \boldsymbol{g_i}(\boldsymbol{x}) \leq \boldsymbol{0} & for\ i = 1, \dots, m \\ \boldsymbol{h_i}(\boldsymbol{x}) = \boldsymbol{0} & for\ i = 1, \dots, l \\ \boldsymbol{x} \in X \end{cases} \tag{6}$$

where $\boldsymbol{f}(\boldsymbol{x})$ is the objective function for the problem, and it is a nonlinear function. $\boldsymbol{g}_i$ and $\boldsymbol{h}_i$ are the constraints for the problem, and $\bar{x}$ is a local optimum point. As this is a nonlinear programming problem, there will be more than one local minimum which needs to be analyzed to decide if it is the real optimum point for the case study.

3.2.1 General economic optimization

The economic optimization problem aims to obtain the optimal point which optimizes the plant economically, and it is determined by an optimizer using the plant model with the most recently updates of measurement adjustments, "$\boldsymbol{\alpha}$", parameters "**β**", constraint limits and economic values. In most RTO applications, the objective function is profit which is given by the product value minus the costs of the operation (DARBY et al., 2011). The optimization problem can be expressed by (7):

$$max\ P(\boldsymbol{x}, \boldsymbol{u}, \boldsymbol{p})$$

$$s.t. \quad \boldsymbol{f}(\boldsymbol{x}, \boldsymbol{u}, \boldsymbol{p}) = 0 \tag{7}$$

$$\max\left(\boldsymbol{x}_{LB}, \boldsymbol{x} - \Delta\right) \leq \boldsymbol{x} \leq \min\left(\boldsymbol{x}_{UB}, \boldsymbol{x} + \Delta\right)$$

in which P is the profit of the process, $\boldsymbol{x}$ are the optimization variables, and there are minimum and maximum limits for each value of $\boldsymbol{x}$. Δ are step limits which represent the maximum change, from the current value, that $\boldsymbol{x}$ is allowed to move in a single optimizer execution. These step limits can cause confusion with interpreting optimizer results. Thus, some implementations automatically solve an additional case to understand the problem without these values (DARBY et al., 2011).

3.3 Mathematical preliminaries to MPA method

The classical RTO method is called Model Parameter Adaptation (MPA).The optimization cycle using MPA method starts with the detection of the steady-state condition in which the process measurements are analyzed in order to decide if the process has reached the SS point based on statistical criteria. If the SS condition is satisfied, the next module is the parameter estimation where the model parameters are used to update the model. Further, these adjustable parameters are used to find the optimal operating point that optimizes the plant economically in the steady-state optimization step. Figure 5 shows the main MPA modules.

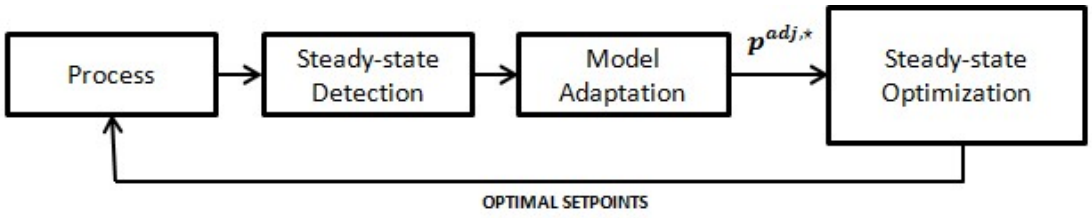

Figure 5 - Main steps in MPA method (Source: Own elaboration).

3.3.1 Steady-state detection

As previously mentioned, the first layer in the MPA cycle is the steady-state detection. The following algorithm is based on Rhinehart and Cao (1995), and it is used in this work as well as in Matias and Le Roux (2018). This algorithm estimates the measurements variance using two different methods and after this, compares them to identify if the process is reasonably steady. The first method estimates the variance between the actual measurement and a filtered tendency of the same value (z_k and $z_{f,k-1}$). The second method calculates the variance between two sequential values (z_k and z_{k-1}). When both of the variances calculated by the two methods are the same, the process can be considered at SS condition. R_{SS} is the variance ratio, and it is equal one when the process is static. The steady-state detection algorithm is represented by (8) - (11).

$$z_{f,k} = \lambda_1 z_k + (1-\lambda_1) z_{k-1} \tag{8}$$

$$\delta^2{}_{1,f,k} = \lambda_2 (z_k - z_{f,k-1})^2 + (1-\lambda_2)\delta^2{}_{1,f,k-1} \tag{9}$$

$$\delta^2{}_{2,f,k} = \lambda_3 (z_k - z_{k-1})^2 + (1-\lambda_3)\delta^2{}_{2,f,k-1} \tag{10}$$

$$R_{SS} = \frac{(2-\lambda_1)\delta^2{}_{1,f,k}}{\delta^2{}_{2,f,k}} \tag{11}$$

where z_k is the given measurement variable ($z_k \in \boldsymbol{y}_{p,k}$) at time t_k and $z_{f,k}$ is the filtered value. $\delta^2{}_{1,f}$ and $\delta^2{}_{2,f}$ are the filtered covariances calculated by the first and the second methods, respectively.

3.3.2 Model adaptation

After it is established that the process is at a steady-state point, the model adaptation module starts in the optimization cycle. In this step, the plant data (SS values) are used to estimate the model parameters by minimizing a weighted sum of squared errors between the measured and predicted outputs (MATIAS and LE ROUX, 2018).

$$\boldsymbol{p}^{\boldsymbol{adj},\star} = \text{argmin} \;\; \Phi_{adap} \coloneqq \|\boldsymbol{y_p} - \boldsymbol{y}\|^2{}_{\boldsymbol{R_p}} \tag{12}$$

$$s.t. \quad G_{adap} \coloneqq \begin{bmatrix} \boldsymbol{0} = \boldsymbol{f}_{ss}\left(\boldsymbol{x}, \boldsymbol{u}, [\boldsymbol{p}^{nom}, \boldsymbol{p}^{adj}]^T\right) \\ \boldsymbol{y} = \boldsymbol{h}\left(\boldsymbol{x}, [\boldsymbol{p}^{nom}, \boldsymbol{p}^{adj}]^T\right) \\ \boldsymbol{p}^{L,adj} \leq \boldsymbol{p}^{adj} \leq \boldsymbol{p}^{U,adj} \end{bmatrix}$$

where $\boldsymbol{p}^{adj}$ are the adjustable parameters, Φ_{adap} is the adaptation problem objective function, $\boldsymbol{R_p}$ are the weights for squared error function, and G_{adap} are the constraints of the model adaptation problem. $\boldsymbol{p}^{L,adj}$ and $\boldsymbol{p}^{\boldsymbol{U},adj}$ are the lower and upper bounds of the adjustable parameters, respectively. $\boldsymbol{p}^{nom}$ are the nominal parameters.

3.3.3 Steady-state optimization

In the MPA and ROPA cycles, the SS optimization uses the adjustable parameters from the online estimation to obtain the optimal setpoint that optimizes the plant economically in the current time. An economic-based problem can be represented by (13):

$$\boldsymbol{u}^{\star} = \text{argmin} \;\; \Phi_{PROFIT}\left(\boldsymbol{u}, \boldsymbol{y}\right) \tag{13}$$

$$s.t. \quad G \coloneqq \begin{bmatrix} \boldsymbol{0} = \boldsymbol{f}_{ss}\left(\boldsymbol{x}, \boldsymbol{u}, [\boldsymbol{p}^{nom}, \boldsymbol{p}^{adj,\star}]\right) \\ \boldsymbol{y} = \boldsymbol{h}\left(\boldsymbol{x}, [\boldsymbol{p}^{nom}, \boldsymbol{p}^{adj,\star}]\right) \\ \boldsymbol{u} \in \boldsymbol{\mathcal{U}} \end{bmatrix}$$

where Φ_{PROFIT} is a scalar economic objective function to be minimized and G is the set of constraints of the problem. The model equation and operational inequalities which are defined by $\boldsymbol{\mathcal{U}} = \{\boldsymbol{u} \in \mathbb{R}^{n_u} : \boldsymbol{u}^L \leq \boldsymbol{u} \leq \boldsymbol{u}^U \wedge \; \boldsymbol{y}^L \leq \boldsymbol{y} \leq \boldsymbol{y}^U\}$ are introduced in G. $\boldsymbol{u}^L, \boldsymbol{u}^U, \boldsymbol{y}^L$ and $\boldsymbol{y}^U$ are the lower and upper bounds of inputs and outputs. Although the optimization problem is formalized as the result of the minimization of the objective function, the aim of this step is to maximize the profit, in practice. After getting the optimal $\boldsymbol{u}^{\star}$, the optimal $y^{\star}$ are obtained in the SS model, and $y^{\star}$ are used as setpoints for the control step which implements the optimal decision for the process.

3.4 Mathematical preliminaries to ROPA method

The ROPA methodology works with three main steps which are shown in the scheme in Figure 6. The ROPA cycle integrates online estimators into the RTO cycle to compute the set of parameters that is used in the steady-state optimization. Hence, ROPA does not depend on the SS detection, and the economic optimization can be done at an arbitrary time. Δt_{ROPA} is the period between two consecutive ROPA executions. After the adjustable parameters ($p^{adj,\star}$) are computed by an online estimator, the economic-based optimization is executed to obtain the optimal setpoints for the plant in the current time (MATIAS and LE ROUX, 2018).

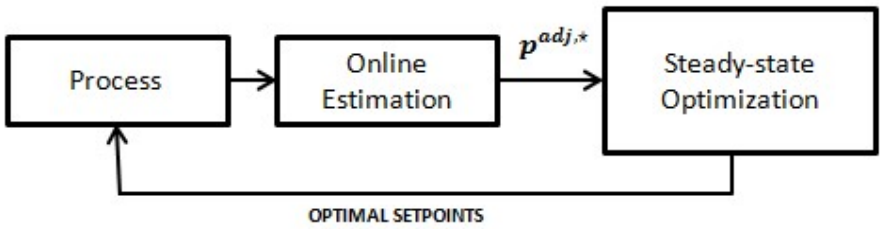

Figure 6 - Main steps in ROPA method (Source: Own elaboration).

3.4.1 Online estimation

As explained before, online estimation is implemented in ROPA method to avoid the problem related to the steady-state wait and the SS detection. In this step, an instrument is used to measure process data, and its inaccuracies generate measurement errors which can cause severe effects on the accuracy of the online estimates. Therefore, a good noise filtration algorithm should be employed to improve the estimation process. The Kalman filter is the optimal state estimator for unconstrained linear systems. The extended Kalman filter (EKF) is an extension of the linear Kalman filter approach, and it is used in nonlinear problems. EKF tries to estimate the states by assuming that the plant model is described by a nonlinear system and the mean and covariance of the measurement errors are known (ASSIS; FILHO, 2000).

3.4.1.1 Extended Kalman Filter – EKF

As previously mentioned, the Kalman filter is the most common choice if the system is linear and there are no constraints on the estimated values. However, as it is difficult to have a linear process in industrial applications, the EKF is more common to be used in practical online estimation. EKF is based on the linearization of the nonlinear plant model, and it takes advantage of the Kalman filter's computational efficiency and recursive strategy (MATIAS and LE ROUX, 2018). The extended Kalman filter has been applied in several systems in the literature. M, P and Jerome (2014) use EKF to estimate the states of a Continuous Stirred Tank reactor (CSTR) to compare it to another type of Kalman filter called unscented Kalman filter (UKF) under various operating conditions and model uncertainties. Prakash, Huang and Shah (2014) also applied EKF in a gas-phase reactor with irreversible reaction system and in an isothermal batch reactor, and two novel schemes of extended Kalman filter are proposed to compare to EKF.

In the ROPA method, the objective is to obtain the states and parameters in the dynamic process at each time instant k. The online estimator needs to infer the most likely values based on the dynamic model and the available sensor measurements. Thus, the dynamic model, represented by (4) and (5), is rearranged resulting in an augmented state $\boldsymbol{x}_k{}^e = [\boldsymbol{x}_k, \boldsymbol{p}_k]^T$, and the parameters are considered additional states. All of the used equations to apply the EKF are based on Matias and Le Roux (2018), and all of them are described as follows.

First, the augmented dynamic system is represented by (14) and (15):

$$\boldsymbol{x}_{k+1}{}^e = \begin{bmatrix} \boldsymbol{f}_{dyn}(\boldsymbol{x}_k, \boldsymbol{u}_k, \boldsymbol{p}_k) \\ \boldsymbol{p}_k \end{bmatrix} + \begin{bmatrix} \boldsymbol{w}_k \\ \boldsymbol{w}_k{}^p \end{bmatrix} = \boldsymbol{f}^e(\boldsymbol{x}_k{}^e, \boldsymbol{u}_k) + \boldsymbol{w}_k{}^e \tag{14}$$

$$\boldsymbol{y}_k = \boldsymbol{h}_k{}^e(\boldsymbol{x}_k{}^e) + \boldsymbol{v}_k \tag{15}$$

where $\boldsymbol{w}_k{}^p \sim \boldsymbol{\mathcal{N}}(\boldsymbol{0}, \boldsymbol{Q}^p)$.

To apply EKF in a system, the linearization of the nonlinear plant model needs to be done. Thus, first-order expansions around the extended state estimate $\hat{\boldsymbol{x}}_{k|k}{}^{e}$ and $\hat{\boldsymbol{x}}_{k|k-1}{}^{e}$ are carried out, and it is represented by (16) and (17). The subscript notation **a**|$\boldsymbol{b}$ means the estimate at time **a** based on information available at time **b**.

$$\boldsymbol{f}^{e}(\boldsymbol{x}_k{}^{e}, \boldsymbol{u}_k) \approx \boldsymbol{f}^{e}\left(\hat{\boldsymbol{x}}^{e}{}_{k|k}, \boldsymbol{u}_k\right) + \boldsymbol{F}_k\left(\boldsymbol{x}_k{}^{e} - \hat{\boldsymbol{x}}^{e}{}_{k|k}\right) \tag{16}$$

$$\boldsymbol{h}^{e}(\boldsymbol{x}_k{}^{e}) \approx \boldsymbol{h}^{e}\left(\hat{\boldsymbol{x}}^{e}{}_{k|k-1}\right) + \boldsymbol{H}_k\left(\boldsymbol{x}_k{}^{e} - \hat{\boldsymbol{x}}^{e}{}_{k|k-1}\right) \tag{17}$$

where:

$$\boldsymbol{F}_k = \frac{\partial \boldsymbol{f}^{e}(\boldsymbol{x}_k{}^{e}, \boldsymbol{u}_k)}{\partial \boldsymbol{x}_k{}^{e,T}}\Big|_{\hat{\boldsymbol{x}}^{e}{}_{k|k}} = \begin{bmatrix} \frac{\partial \boldsymbol{f}(\boldsymbol{x}_k, \boldsymbol{u}_k, \boldsymbol{p}_k)}{\partial \boldsymbol{x}_k{}^{T}} & \frac{\partial \boldsymbol{f}(\boldsymbol{x}_k, \boldsymbol{u}_k, \boldsymbol{p}_k)}{\partial \boldsymbol{p}_k{}^{T}} \\ \boldsymbol{0} & \boldsymbol{I}_{np} \end{bmatrix}_{\hat{\boldsymbol{x}}^{e}{}_{k|k}} \tag{18}$$

and

$$\boldsymbol{H}_k = \frac{\partial \boldsymbol{f}^{e}(\boldsymbol{x}_k{}^{e})}{\partial \boldsymbol{x}_k{}^{e,T}}\Big|_{\hat{\boldsymbol{x}}^{e}{}_{k|k-1}} = \begin{bmatrix} \frac{\partial \boldsymbol{h}(\boldsymbol{x}_k, \boldsymbol{p}_k)}{\partial \boldsymbol{x}_k{}^{T}} & \frac{\partial \boldsymbol{h}(\boldsymbol{x}_k, \boldsymbol{p}_k)}{\partial \boldsymbol{p}_k{}^{T}} \end{bmatrix}_{\hat{\boldsymbol{x}}^{e}{}_{k|k-1}} \tag{19}$$

in which I_{np} is the identity matrix with dimension np.

After the linearization of the plant model, the EKF equations can be directly applied. In the prediction step, the nonlinear model is used instead of using linear approximation as shown in (20):

$$\hat{\boldsymbol{x}}^{e}{}_{k+1|k} = \boldsymbol{f}^{e}\left(\hat{\boldsymbol{x}}^{e}{}_{k|k}, \boldsymbol{u}_k\right) \tag{20}$$

The EKF prediction and update equations are represented by (21), (23), and the gain of Kalman filter is computed by (22), as follows:

$$\boldsymbol{P}_{k+1|k} = \boldsymbol{F}_k \boldsymbol{P}_{k|k} \boldsymbol{F}_k{}^{T} + \boldsymbol{Q}^{e} \tag{21}$$

$$\boldsymbol{K}_{k+1} = \boldsymbol{P}_{k+1|k} \boldsymbol{H}^{T}{}_{k+1} [\boldsymbol{H}_{k+1} \boldsymbol{P}_{k+1|k} \boldsymbol{H}^{T}{}_{k+1} + \boldsymbol{R}]^{-1} \tag{22}$$

$$\boldsymbol{P}_{k+1|k+1} = \boldsymbol{P}_{k+1|k} - \boldsymbol{K}_{k+1}\boldsymbol{H}_{k+1}\boldsymbol{P}_{k+1|k} \tag{23}$$

with

$$\boldsymbol{Q}^{e} = \begin{bmatrix} \boldsymbol{Q} & \boldsymbol{0} \\ \boldsymbol{0} & \boldsymbol{Q}^{p} \end{bmatrix}$$

The extended states are estimated using the prediction error:

$$\widehat{\boldsymbol{x}}^{e}{}_{k+1|k+1} = \widehat{\boldsymbol{x}}^{e}{}_{k+1|k} + \boldsymbol{K}_{k+1}[\boldsymbol{y}_{k+1} - \boldsymbol{h}^{e}(\widehat{\boldsymbol{x}}^{e}{}_{k+1|k})] \tag{24}$$

4 CASE STUDY 1: WILLIAMS-OTTO REACTOR

This Chapter discusses the application of the Real-time Optimization with Persistent Adaptation (ROPA) and the Model Parameter Adaptation (MPA) method to the Williams-Otto reactor problem. The main objectives are to reproduce the ROPA and MPA algorithms and to show the benefits of using ROPA in the RTO cycle comparing both of the methods. MPA uses the steady-state data to optimize the plant economically while ROPA uses transient information.

The results show that the integration of RTO with online estimators can predict the states and parameters satisfactorily even with disturbances in the system since the steady-state detection layer is not necessary, and the period between two optimization executions is shorter than in other RTO methods which need this step. Moreover, the computed solution tends to the stationary plant optimum. The advantages of using ROPA are discussed in this Chapter.

4.1 The process model

The assumptions for the case study are based on Matias and Le Roux (2018). The Williams-Otto reactor is widely used for RTO and control studies. A flow diagram is shown in Figure 7.

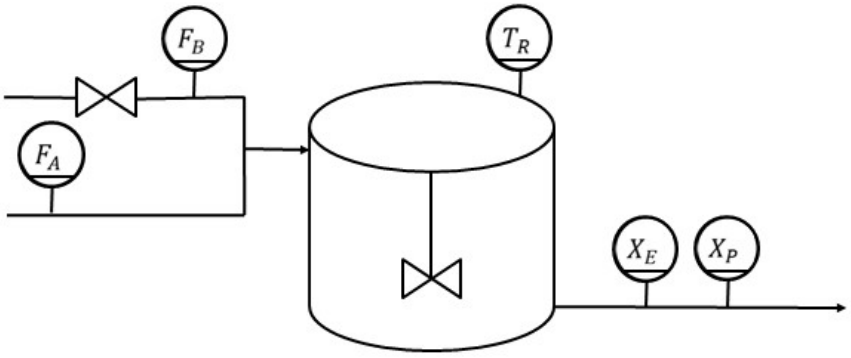

Figure 7 - Williams-Otto reactor scheme (Source: MATIAS and LE ROUX, 2018).

The process is fed with the two feed streams which are composed of pure A and B. There are two products of interest: P and E. Also, there are an undesired

product G, and an intermediate C. The set of reactions in the process can be seen as follows:

r_1: $A + B \overset{k_1}{\rightarrow} C$

r_2: $B + C \overset{k_2}{\rightarrow} P + E$

r_3: $C + P \overset{k_3}{\rightarrow} G$

The assumptions for the problem are described as follows: the reactor is represented by an ideal continuous stirred-tank reactor (CSTR), and the temperature of the reactor can be changed without cost and instantaneously, discarding the energy balances in the model. With these assumptions, the steady-state and dynamic models are created. The dynamic model is shown below. The SS model is not shown here because it can be easily derived from the dynamic model.

$$
\begin{aligned}
0 &= F_R - F_A - F_B \\
\frac{dX_A}{dt} &= f_{dyn,1}(\boldsymbol{X}, \boldsymbol{u}) = \frac{(F_A - F_R X_A)}{M_t} - k_1 X_A X_B \\
\frac{dX_B}{dt} &= f_{dyn,2}(\boldsymbol{X}, \boldsymbol{u}) = \frac{(F_B - F_R X_B)}{M_t} - k_1 X_A X_B - k_2 X_B X_C \\
\frac{dX_C}{dt} &= f_{dyn,3}(\boldsymbol{X}, \boldsymbol{u}) = \frac{(-F_R X_C)}{M_t} + 2k_1 X_A X_B - 2k_2 X_B X_C - k_3 X_C X_P \\
\frac{dX_E}{dt} &= f_{dyn,4}(\boldsymbol{X}, \boldsymbol{u}) = \frac{(-F_R X_E)}{M_t} + 2k_2 X_B X_C \\
\frac{dX_P}{dt} &= f_{dyn,5}(\boldsymbol{X}, \boldsymbol{u}) = \frac{(-F_R X_P)}{M_t} + k_2 X_B X_C - 0.5 k_3 X_C X_P \\
\frac{dX_G}{dt} &= f_{dyn,6}(\boldsymbol{X}, \boldsymbol{u}) = \frac{(-F_R X_G)}{M_t} + 1.5 k_3 X_C X_P \\
k_i &= A_i e^{-E_i/T_R}, \quad i = 1, \ldots, 3
\end{aligned}
\tag{25}
$$

where k_i, A_i, and E_i are the reaction rate constant, frequency factor, and the activation energy for reaction i; M_t is the reactor mass holdup which is assumed constant, and X_j and F_j are the mass fraction and mass flow rate of component j. The mass flow rate of reactant A, F_A, is fixed and the manipulated variables of the system are the flow of reactant B, F_B, and the reactor temperature, T_R.

The stationary model is used in the economic optimization layer in the ROPA and MPA cycles. It is also used in the model adaptation step during the MPA cycle. On the other hand, the dynamic model is used as a representation of the plant and for linearization purposes. In respect of the model parameters, although the selection of adjustable set is composed of the frequency factors and activation energies of reactions, a parameter rearrangement was carried out in order to avoid a poorly conditioned parameter estimation problem, as done in Matias and Le Roux (2018) and shown in (26).

$$\begin{aligned} &\ln(k_i) = \Phi_i + \left(\frac{T_{ref}}{T_R} - 1\right)\Psi_i, \qquad i = 1, \dots, 3 \\ &\Phi_i = \log(A_i) + \Psi_i \\ &\Psi_i = -\frac{E_i}{T_{ref}} \end{aligned} \tag{26}$$

where Φ_i and Ψ_i are the rearranged parameters of i^{th} reaction and T_{ref} = 383.15 K. Thus, the model summary for this process can be described as follows:

$$\begin{aligned} &\boldsymbol{x} = [X_A, X_B, X_C, X_E, X_P, X_G]^T \\ &\boldsymbol{y} = [X_E, X_P]^T \\ &\boldsymbol{u} = [F_B, T_R]^T \\ &\boldsymbol{p} = [p_1, p_2, p_3, p_4, p_5, p_6]^T = [\Phi_1, \Psi_1, \Phi_2, \Psi_2, \Phi_3, \Psi_3]^T \end{aligned} \tag{27}$$

where $\boldsymbol{x}$ is the vector of the complete system model states, $\boldsymbol{y}$ is the vector of the measurements, $\boldsymbol{u}$ is the vector of the decision variables, and $\boldsymbol{p}$ is the vector of the adjustable parameters.

The initial plant condition and the nominal values of the parameters are listed in Table 1.

Table 1 - Initial plant condition and adjustable parameter set of Williams-Otto model. The values are based on Matias and Le Roux (2018). The lower and upper bounds of the manipulated variables and the parameters are used in the economic optimization layer in the ROPA and MPA cycles.

	Variable(symbol) [unit]	Lower bound	Initial value	Upper bound
-	Reactor holdup (M_t) [Kg]	-	2105	-
-	Flow of reactant A (F_A)[Kg/s]	-	1.827	-
$\boldsymbol{u_1}$	Flow of reactant B (F_B)[Kg/s]	4	4.787	6
$\boldsymbol{u_2}$	Reactor temperature (T_R)[ºC]	80	89.70	100
$\boldsymbol{x_1}$	Mass fraction of A (X_A)[-]	-	0.0876	-
$\boldsymbol{x_2}$	Mass fraction of B (X_B)[-]	-	0.3892	-
$\boldsymbol{x_3}$	Mass fraction of C (X_C)[-]	-	0.0153	-
$\boldsymbol{x_4/y_1}$	Mass fraction of E (X_E)[-]	-	0.1093	-
$\boldsymbol{x_5/y_2}$	Mass fraction of P (X_P)[-]	-	0.2903	-
$\boldsymbol{x_6}$	Mass fraction of G (X_G)[-]	-	0.1083	-
$\boldsymbol{p_1}$	Φ_1[-]	-3.385	-3.077	-2.769
$\boldsymbol{p_2}$	Ψ_1[-]	-18.26	-17.39	-14.78
$\boldsymbol{p_3}$	Φ_2[-]	-1.826	-1.353	-1.217
$\boldsymbol{p_4}$	Ψ_2[-]	-22.83	-21.74	-17.39
$\boldsymbol{p_5}$	Φ_3[-]	-0.5188	-0.3843	-0.3459
$\boldsymbol{p_6}$	Ψ_3[-]	-30.44	-28.99	-27.54

4.2 Economic Optimization

For this case study, the objective in this layer is to maximize the unit profit, Φ_{profit}. Thus, the objective function in the optimization problem is the profit, and it can be described as in (28).

$$\Phi_{profit} = 1143.38X_P F_R + 25.92X_E F_R - 76.23F_A - 114.34F_B \quad (28)$$

The components E and P are the valuable products, and the numerical values in the equation are the market prices of these components as well as the purchasing values of the reactants A and B (all prices are in $\$/Kg$). X_P and X_E are the mass fractions of P and E, respectively. Moreover, the economic optimization is a

constrained optimization problem where the set of constraints is composed of the model equations and operational inequality constraints.

4.3 Process Simulation

The process simulations are performed in MATLAB, and the dynamic system is solved by SundialsTB (HINDMARSH et al., 2005) using the *CVode* function. Moreover, the sensitivities are calculated by SundialsTB. The information flow between layers in the ROPA and MPA cycles can be seen in Figure 8 below.

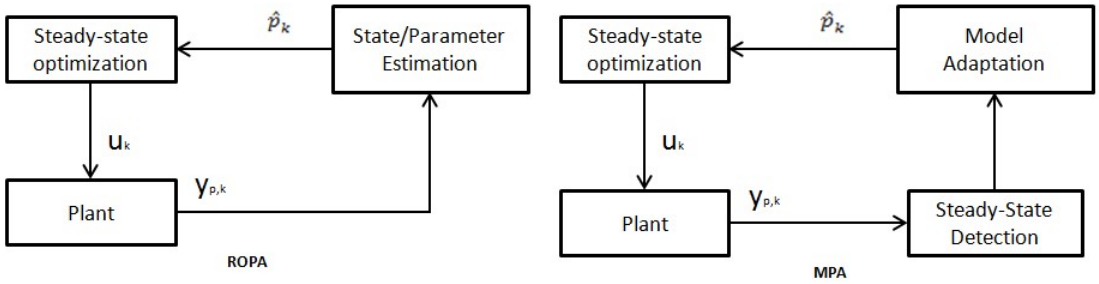

Figure 8 - ROPA and MPA information flows (Source: Adapted from MATIAS and LE ROUX, 2018).

In this case study, the plant measurements, $y_{p,k}$, are the mass fraction of components E and P in the current time, and they are obtained using a sensor that is simulated. Subsequently, these values are used in the estimation layers in order to estimate the states and parameters in the process. $\hat{p}_k$ are the estimated parameters, and they are estimated using the Extended Kalman filter (EKF) in the ROPA method and the model adaptation problem in the MPA cycle. Finally, the vector with the optimal values of the decision variables, u_k, is sent to the plant. The implementation of a model predictive control (MPC) layer can be done before this last step, but it is not mandatory.

In order to simulate a real plant, random and deterministic disturbances were admitted in the system. The noisy plant measurements, y_1 and y_2, are obtained by adding random disturbances to the outputs of the dynamic model, as shown in (29).

$$y_{n,k} = y_k + error \,.\, y_k \,.\, randn() \tag{29}$$

where $y_{n,k}$ is the measurement with noise at time k; y_k is its actual value; the $error$ is equal to 1%; and $randn$ draws a random scalar from the standard normal distribution.

The process is also affected by deterministic disturbances which can be divided into measured and unmeasured. The measured disturbance affects the flow rate of reactant A, F_A, and the unmeasured disturbance changes the nominal values of the parameters of the second and third reactions.

After 10 h, a step change of 0.173 kg/s to the nominal value of F_A is added. This value remains disturbed until 15 h. Also, the reaction parameters $(\Phi_2, \Psi_2, \Phi_3, \Psi_3)$ are affected by the unmeasured disturbance, changing from their nominal values (shown in Table 1) to [-1.642, -22.0391, -0.3582, -28.9730] between 18 h and 21 h. After this, they start to return their nominal values.

As mentioned before, an online estimator is used in the ROPA cycle aiming to estimate the states and parameters in the current time. In this process, the Extended Kalman filter (EKF) is used in the estimation layer using (21) - (24). The filter tuning parameters used for EKF are shown below:

$$\begin{aligned} \boldsymbol{Q} &= diag([1e^{-1};\ 1e^{-1};\ 1e^{-1};\ 1e^{-2};\ 1e^{-2};\ 1e^{-2}]) \\ \boldsymbol{Q^p} &= diag([1e^{1};\ 0.4e^{3};\ 1e^{1};\ 0.2e^{3};\ 1e^{0};\ 0.5e^{2}]) \\ \boldsymbol{R} &= diag([1e^{1};\ 1e^{1}]) \end{aligned} \tag{30}$$

where $\boldsymbol{Q}$, the covariance matrix of the process model, is related to the states $(X_A, X_B, X_C, X_E, X_P, X_G)$; $\boldsymbol{R}$, the measurement noise covariance matrix, is related to the measured variables (X_E, X_P); and $\boldsymbol{Q^p}$, the parameter covariance matrix, corresponds to the parameters $(\Phi_1, \Psi_1, \Phi_2, \Psi_2, \Phi_3, \Psi_3)$. The values of $\boldsymbol{Q}$, $\boldsymbol{R}$ and $\boldsymbol{Q^p}$ are kept constants during the RTO implementations. Moreover, the weighting factor for the model adaptation algorithm, $\boldsymbol{R}_P$, is the identity matrix.

Also, the period between two optimization executions, Δt_{ROPA}, is another important tuning parameter in the simulations. This value needs to have a similar order of magnitude as the process settling time. However, it should be large enough to capture the disturbances. For the case study, a $\Delta t_{ROPA} = 10\,min$ was chosen to simulate the process.

Regarding the MPA method, the first step is the steady-state detection in which the filter values for each measured variable are tuned according to the arrays below.

$\boldsymbol{\lambda}_1 = [0.2, 0.3]$, $\boldsymbol{\lambda}_2 = [0.1, 0.2]$, $\boldsymbol{\lambda}_3 = [0.1, 0.2]$, $\boldsymbol{R}_{crit} = [2.5, 2.5]$

where the first and second values of the arrays are related to the component E and P, respectively. All of these values are also based on Matias and Le Roux (2018).

The economic steady-state optimization was done using the *fmincon* function in MATLAB for both of the RTO methods. The interior-point algorithm which is the default algorithm for *fmincon* function was used in the optimization executions. Moreover, the gradient of the objective function (profit) was set in the code manually to get better solution for the problem.

4.4 Results and discussion

The ROPA and MPA performances are analyzed by the states and parameters estimation in the simulations as well as the economic results. As ROPA uses transient information in the estimation layer, these values need to be reliable at the current time. Thus, the choice of the online estimator must be carefully done, and the results require a rigorous analysis. The use of transient data to update the model in a dynamic process ensures that the economic optimization does not stop when the process is under disturbances. Hence, the steady-state (SS) wait issue is no longer a problem, and the detection of the SS condition is not necessary anymore. The ROPA is executed every Δt_{ROPA} instants resulting in a short period between two sequential optimization executions, hence the ROPA estimation capacity under disturbances enhances when compared to the other RTO methods which require the SS detection step. Regarding the MPA method, the SS detection step is necessary in which the economic optimization runs only when the process is at the SS condition. Thus, in case a disturbance affects the system, the optimization cycle needs to wait for the next steady-state point to return the calculations.

The dynamic model is solved by SundialsTB in order to obtain the state profiles as shown in Figure 9. The initial plant condition, shown in Table 1, is used to simulate the process. Moreover, random and deterministic disturbances are considered aiming to handle with a real plant. These values are used as the plant values in the optimization cycle.

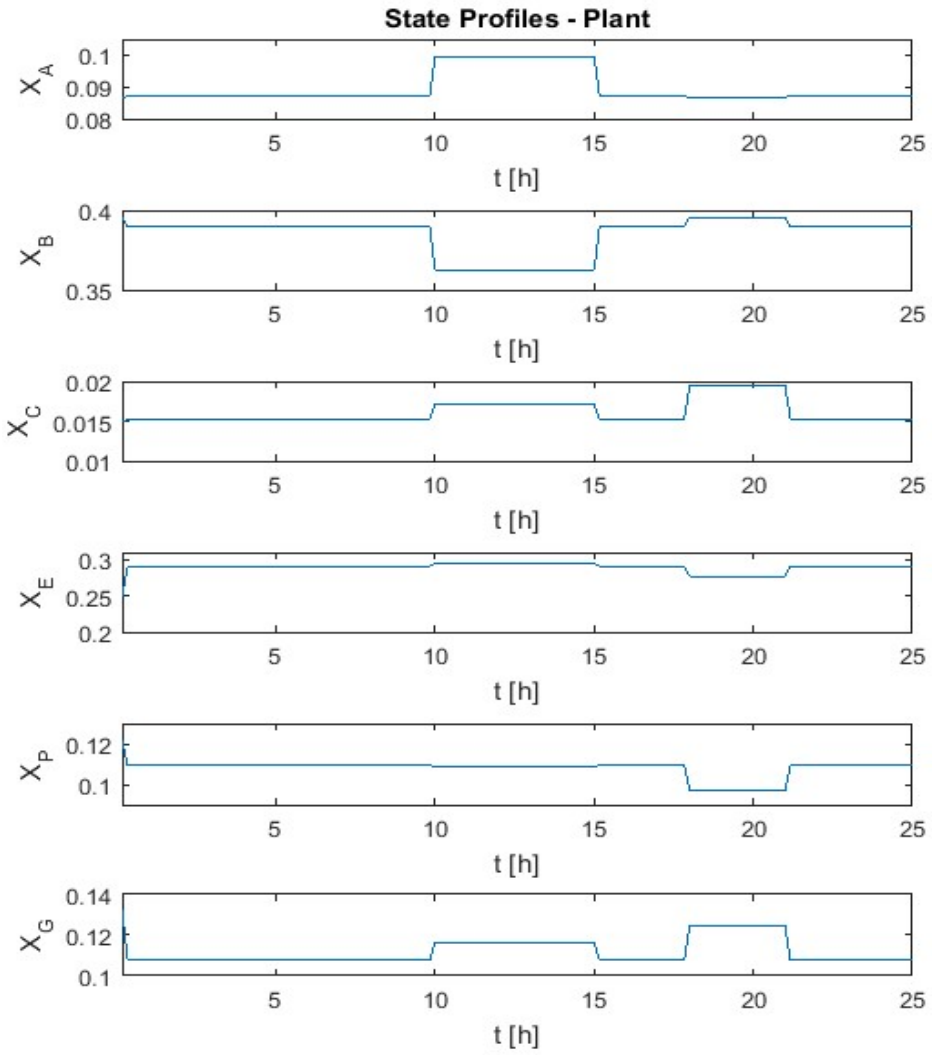

Figure 9 - Plant condition calculated by SundialsTB (Source: own elaboration).

The first estimation analysis is the state estimation. In both of the RTO methods, ROPA and MPA, the Extended Kalman filter (EKF) is chosen to be the online state estimator since the model is nonlinear. Figure 10 shows the state estimation for ROPA and MPA cycles as well as for the plant (optimal value). X_E and X_P are not shown because they are assumed to be directly measured in the plant instead of being estimated by the filter.

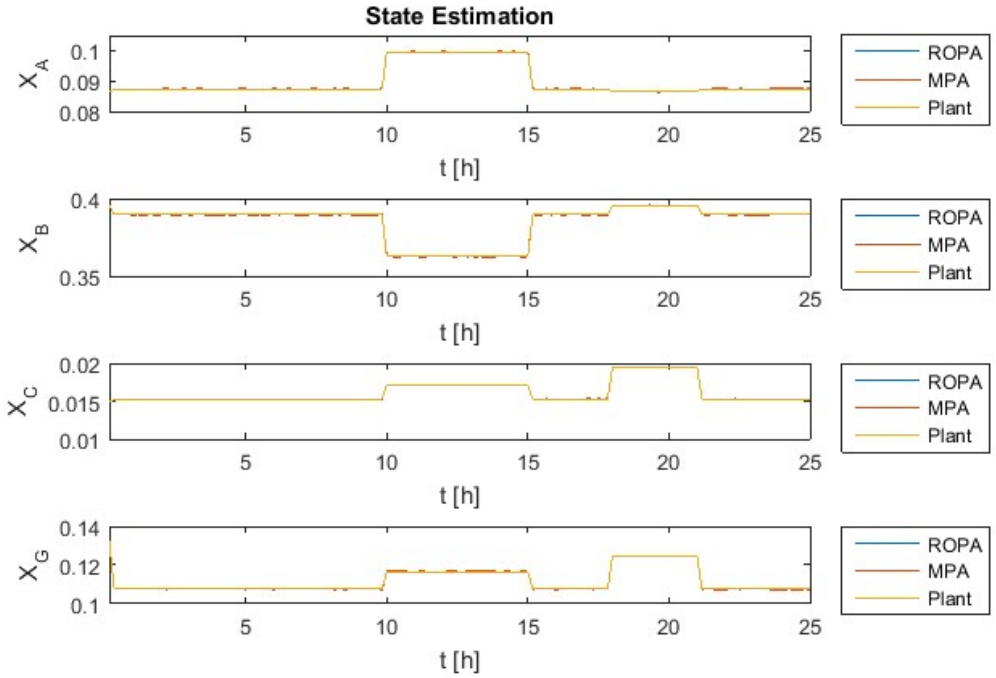

Figure 10 – State estimation for ROPA and MPA implementations in the Williams-Otto reactor using the Extended Kalman filter as the online estimator (Source: own elaboration).

Regarding the state estimation, the estimated and actual state profiles are almost overlapped in the given time horizon for ROPA and MPA methods. These values are similar because the considered disturbances affecting the system are equivalent for both of the methods. The results show that the filter works consistently, and the state covariance matrix is satisfactorily tuned by Matias and Le Roux (2018) . Although it is not the main focus of the case study, if a model predictive control (MPC) is added in the system, the filter should satisfactorily predict the states since these values are used as feedback to the MPC layer.

The parameter estimation for ROPA and MPA implementations is shown in Figure 11 below. The estimated parameter values are compared to the actual plant values. It is possible to notice that even with the disturbances which affect the parameters p_3, p_4, p_5 and p_6 the ROPA method estimate the parameters correctly. Clearly, the MPA parameter estimates are unreliable since MPA does not follow the plant condition as ROPA. Moreover, there is a delay related to the MPA method to estimate the parameters p_3, p_4 and p_5. It is due to the fact that the classical method needs to wait for the next SS condition to start the optimization cycle after a disturbance in the system. The gap between the disturbance occurrence and the

response of MPA is almost three hours what highlights the critical issue related to this methodology, the steady-state wait. Thus, the estimates for MPA method are updated only after this response that takes a longer time when compared to the ROPA method which does not need to wait for the next SS point. The parameter estimation shows that ROPA is able to respond to the disturbances occurrence reproducing the actual plant parameter profile (the lines are almost overlapped). The most critical advantage of ROPA is that it can update the model even under disturbances.

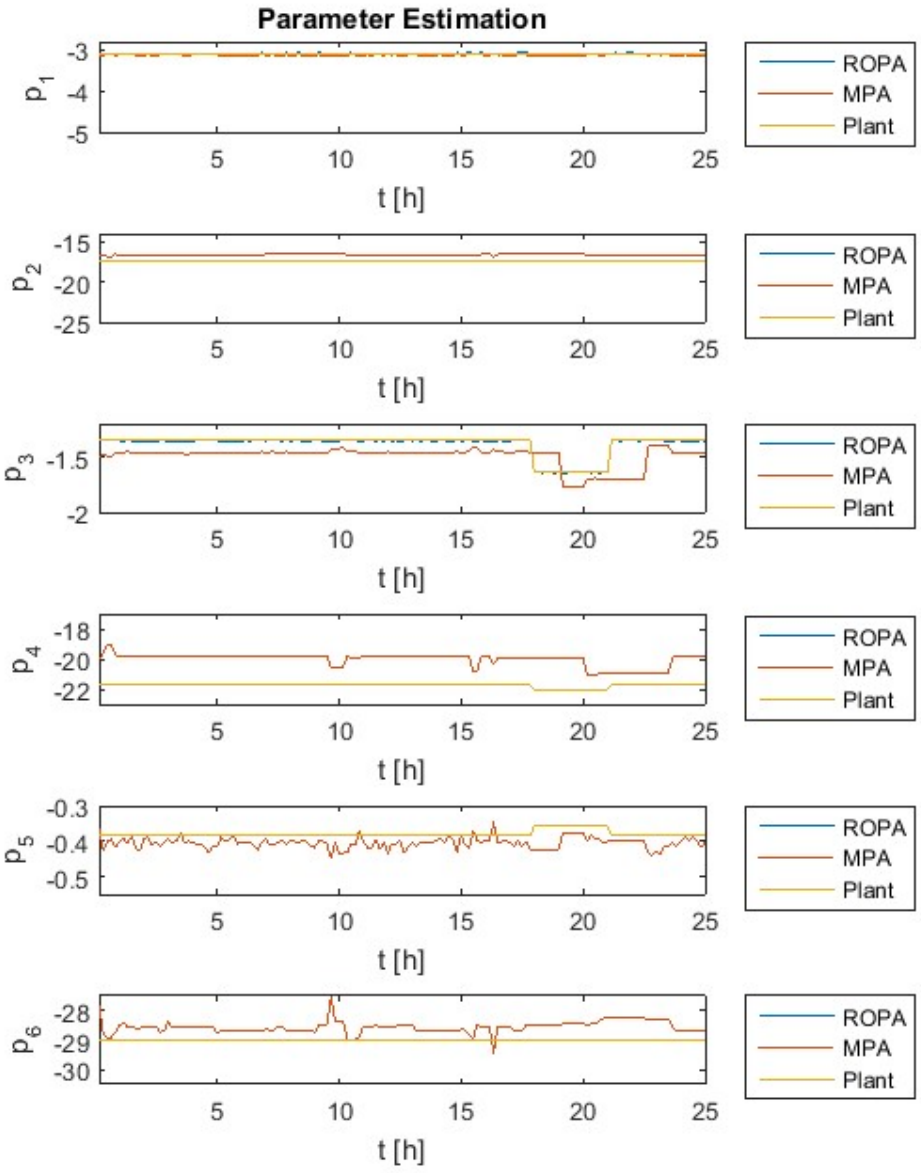

Figure 11 - Estimated parameters for ROPA and MPA implementations in the Williams-Otto reactor (Source: own elaboration).

In the optimization cycle, a process with identifiability problem can have different set of adjustable parameters ($\boldsymbol{p}^{adj}$) which result in the same optimum values for the problem. This problem occurs when the Hessian matrix of the problem is ill-conditioned, so the process has identifiability problems, and the estimation affects the performance of the optimizer. Since the Williams-Otto reactor presents identifiability issues (MATIAS and LE ROUX, 2018), the analysis of the parameter estimation may not be the only result to be used to assess the methods' performance. Moreover, it is not enough to conclude if the result of the optimization is the real plant optimum. However, the assumptions that there is only a unique optimum solution for the SS optimization ($\boldsymbol{u}^{\star}$) and that this solution matches the true plant parameter values are used in the case study, as in Matias and Le Roux (2018). Additionally, there is no plant-model mismatch (the model can be considered perfect). The ROPA and MPA convergence analysis is based on these assumptions.

A proper indicator when the system presents identifiability problems are the economic performance of the closed-loop optimization and the optimal decisions since the parameter estimation result cannot be conclusive. The analysis of the economic performance is used to evaluate the ROPA and MPA implementations. The instantaneous profit is shown in Figure 12 for both of the methodologies. It can be observed that the response of ROPA follows the optimal instantaneous profit, even after the disturbances in the system. Although bias between the optimal value and the value obtained with ROPA methodology can be detected during the simulations, ROPA runs the economic optimization continuously independently of the plant condition. Clearly, the response of ROPA is faster for both of the disturbances (measured and unmeasured). ROPA performance shows that the method can properly converge to the stationary optimum. As in the parameter estimation results, a delay is detected in the MPA implementation. MPA has an inherent delay on the optimization cycle due to the steady-state detection. The MPA optimization runs only after the system reaches the next SS. Furthermore, MPA economic results drift from the optimal profit (plant). The decision variables of the ROPA and MPA cycles can be compared to the plant optimal decisions, as shown in Figure 13. It can be seen that the decision variables calculated by ROPA method move towards the optimal values, even with the disturbances in the system. For the MPA cycle, the decision variables also present a delay due to the SS detection layer.

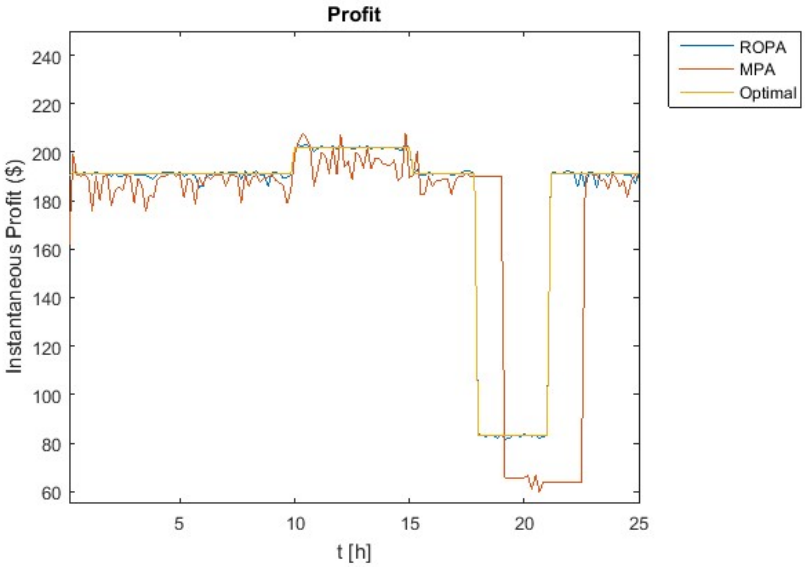

Figure 12 – Comparison between the instantaneous profit of the ROPA and MPA methods for the Williams-Otto reactor study (Source: own elaboration).

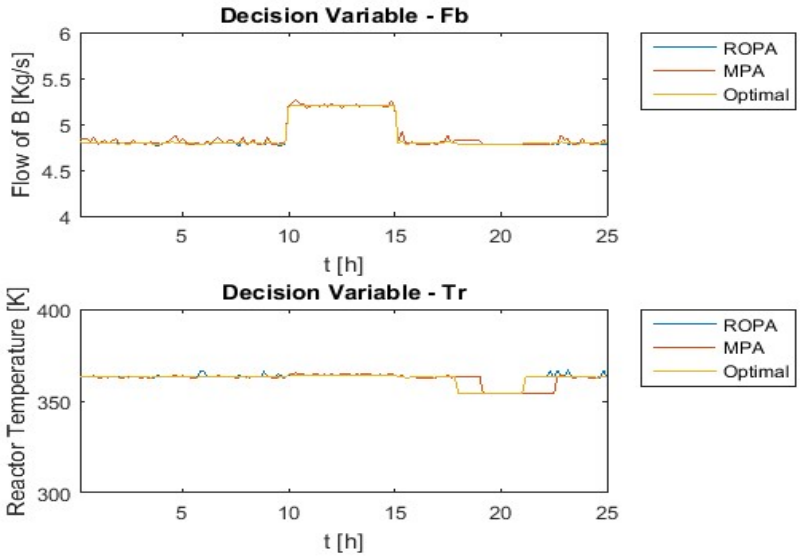

Figure 13 - Comparison between the plant optimal decisions and the inputs calculated by ROPA and MPA implementations in the Williams-Otto reactor (Source: own elaboration).

In order to obtain more information about the distribution of the economic performance for MPA and ROPA methods and the influence of the critical value (R_{crit}) in the MPA algorithm, Monte Carlo analyses are performed. 100 repetitions of the simulations are executed in each scenario for ROPA and MPA. Two different scenarios are used in the simulations aiming at analyzing the economic performance for both methods: (**Scenario 1**) disturbances in F_A and the nominal parameters p_3, p_4, p_5 and p_6, and (**Scenario 2**) disturbances in F_A and the nominal parameter p_3. Furthermore, three different scenarios are used to obtain more information about the

influence of R_{crit} in the MPA cycle: (**Scenario 3**) $R_{crit} = 2.0$; (**Scenario 4**) $R_{crit} = 2.5$; (**Scenario 5**) $R_{crit} = 3.0$. The disturbances in scenario 1 are used for the second Monte Carlo analysis, varying the R_{crit} value in the MPA algorithm. Although the ROPA algorithm does not change with the R_{crit} value, the ROPA results in the second Monte Carlo analysis are shown to compare both MPA and ROPA for all of the scenarios 3, 4 and 5. The frequency distribution of the profit calculated using MPA and ROPA methods and the true profit value (vertical line) for each scenario is shown in Figure 14 and Figure 15.

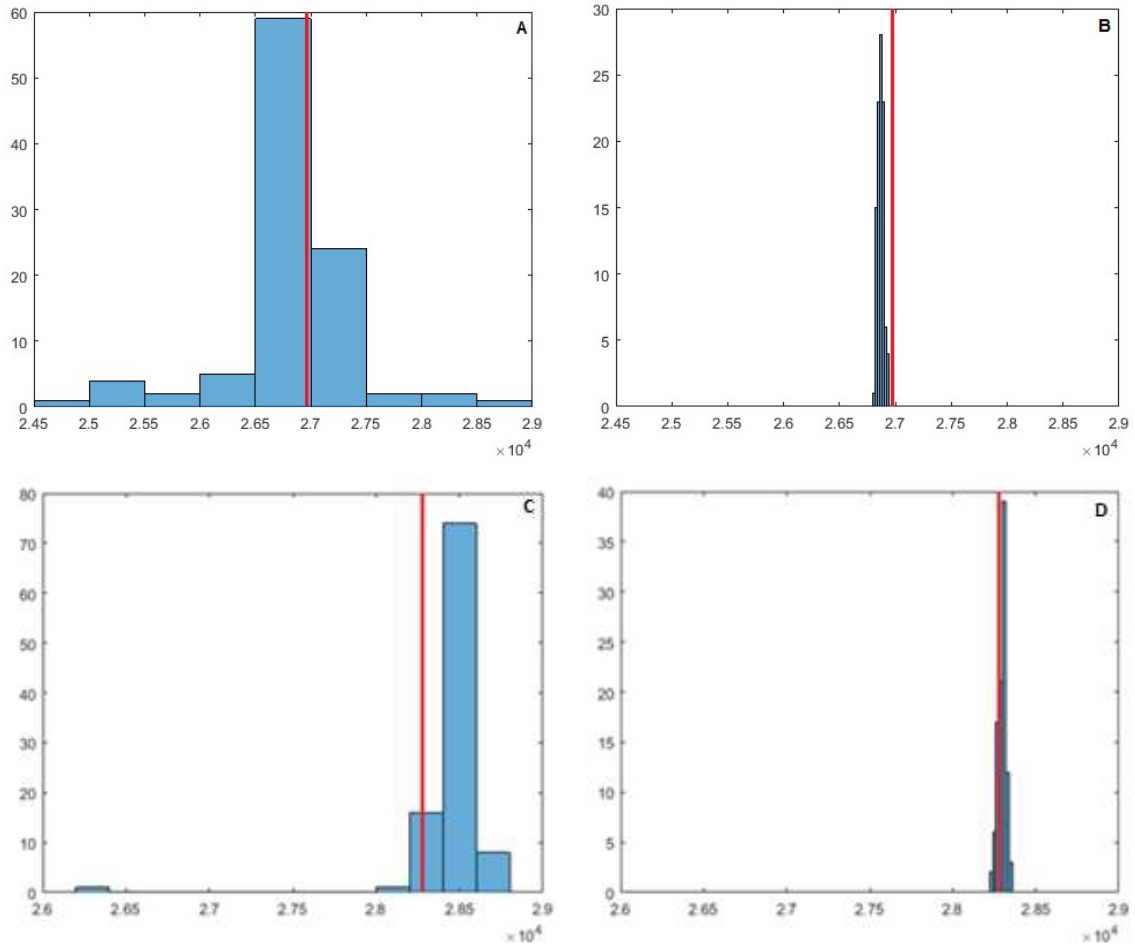

Figure 14 - Monte Carlo Analysis - Frequency distribution of the profit calculated using MPA and ROPA methods and the true profit value (vertical line) for each scenario in the Williams-Otto reactor. (A) Scenario 1 calculated using MPA method; (B) Scenario 1 calculated using ROPA method; (C) Scenario 2 calculated using MPA method; (D) Scenario 2 calculated using ROPA method.

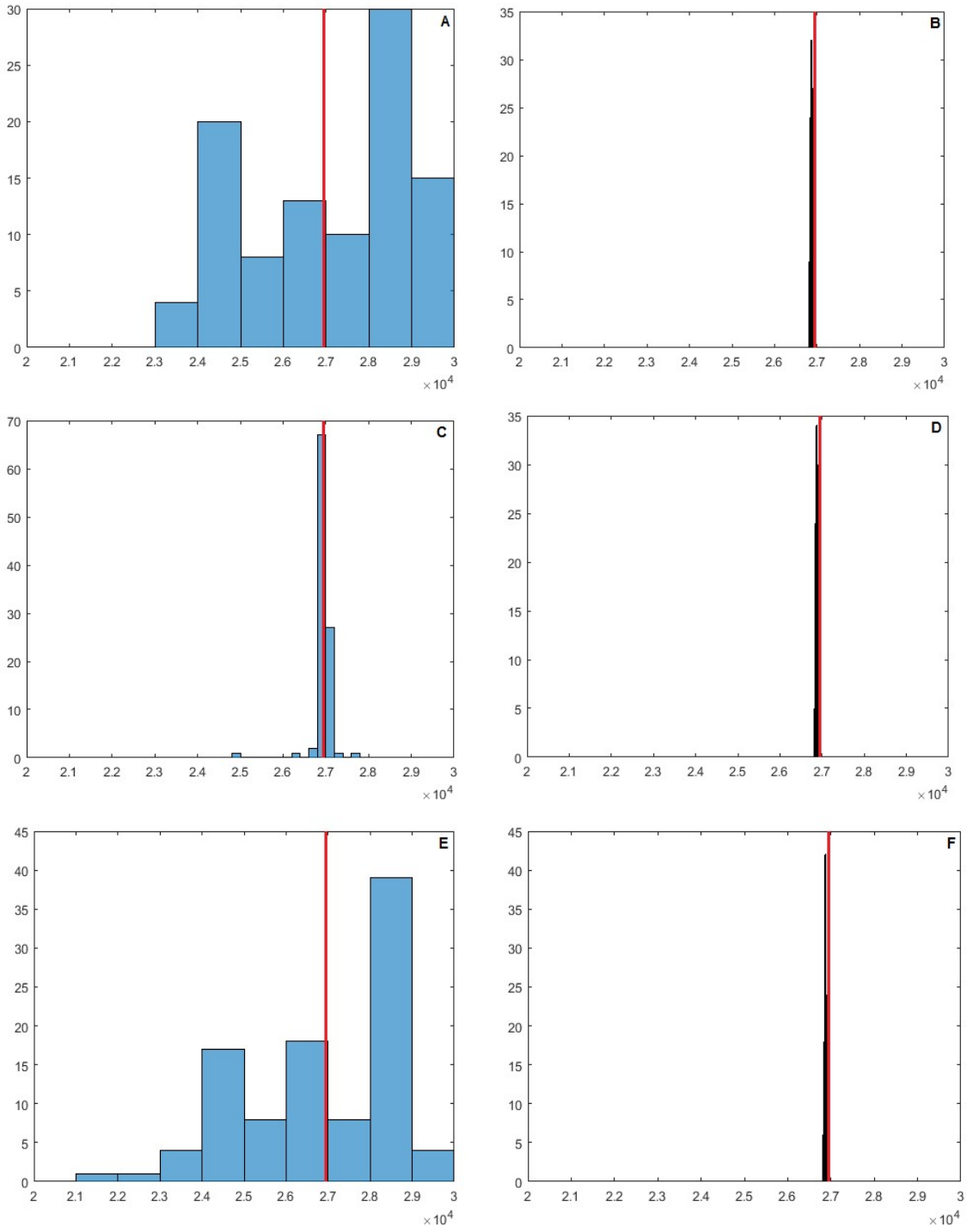

Figure 15 - Monte Carlo Analysis - Frequency distribution of the profit calculated using MPA and ROPA methods and the true profit value (vertical line) for each scenario in the Williams-Otto reactor. (A) Scenario 3 ($R_{crit} = 2.0$) calculated using MPA method; (B) Scenario 3 ($R_{crit} = 2.0$) calculated using ROPA method; (C) Scenario 4 ($R_{crit} = 2.5$) calculated using MPA method; (D) Scenario 4 ($R_{crit} = 2.5$) calculated using ROPA method; (E) Scenario 5 ($R_{crit} = 3.0$) calculated using MPA method; (F) Scenario 5 ($R_{crit} = 3.0$) calculated using ROPA method.

For the first Monte Carlo analysis, scenarios 1 and 2, it can be seen that the MPA method results change more significantly than ROPA during the 100 iterations considering the same range of profit values. It can be due to the fact that MPA uses a statistical algorithm which may change with random influences. Regarding the second Monte Carlo analysis, Scenario 4 ($\mathrm{R_{crit}} = 2.5$) is chosen to be in line with the value in Matias and Le Roux (2018), and this Monte Carlo analysis shows it is a good choice when compared to values of $\mathrm{R_{crit}} = 2.0$ and $\mathrm{R_{crit}} = 3.0$ since the MPA result that does not change as in scenarios 3 and 5 using the same range of profit values. ROPA results also vary in all of the scenarios due to the random disturbances added to the outputs of the process.

In conclusion, the integration of RTO with online estimator enhances the estimation capacity of the problem and the disturbance detection, and improves the economical issue when compared to the classical RTO method (MPA) because the period between two optimization iterations is shorter than in the MPA method which requires the SS detection (there is an increase of the model updating frequency). Also, ROPA does not have the steady-state wait problem since it uses transient data which are always available.

4.5 Conclusions

The Real-time Optimization with Persistent Adaptation (ROPA) method integrates transient data to the static optimization. In ROPA cycle, online estimators are used to obtain the transient data in the current time. If the model is nonlinear, the Extended Kalman filter (EKF) can be used to estimate the states and parameters that are used to update the model. As the plant, represented by the dynamic model, is subjected to disturbances, the use of transient information improves the prediction capacity of the RTO method. The detection of the SS condition layer is not necessary in the ROPA cycle since it runs the optimization each Δt_{ROPA} independently of the plant condition. Therefore, the period between two optimization executions decreases when compared to the MPA method that requires the SS detection. With this, the estimation capacity and the disturbances detection increase in the optimization cycle.

Since the state and parameter estimation capacity in the ROPA cycle increases when compared to the MPA method, it can satisfactorily reproduce the

actual plant profile which improves the economic optimization. The results show that ROPA reaches the stationary plant optimum even using transient data in a SS optimization, and the EKF works consistently. However, it is important to highlight that the plant needs to be well tuned to get suitable results for the optimization problem. The tuning phase may be properly done in the ROPA cycle. Otherwise, the process cannot be optimized correctly.

ROPA is an intermediary solution between the static RTO (as MPA) and the dynamic optimization (DRTO/EMPC). ROPA constantly improves the plant operations if the tuning parameters are well-established. The main contribution of this study is to show evidences that the ROPA implementation in processes can converge to the stationary plant optimum, even using transient data to update the model in a steady-state optimization. ROPA applications can show this convergence and provide the benefits of using the method instead of using the classical RTO method (MPA). In the Williams-Otto reactor study, ROPA converges to the steady-state plant optimum even using dynamic data to update the model, and it is compared to the MPA method which has an inherent delay due to the steady-state detection. The results of the comparison show that the decrease in the execution frequency (the time between two sequential optimization cycles) enhances the economic optimization for the considered case study.

5 CASE STUDY 2: PROPYLENE CHLORINATION PROCESS

This Chapter shows the results of the application of the Real-time Optimization with Persistent Adaptation (ROPA) and the Model Parameter Adaptation (MPA) methods to a gas-phase Continuous Stirred Tank reactor (CSTR). The results of the case study are analyzed in order to compare ROPA and MPA methodologies. ROPA works with transient data to update the plant model in the RTO cycle using online estimator. On the other hand, MPA uses steady-state data to estimate the parameters in the optimization problem. The main issue related to the MPA method is the time the process spends to reach the steady-state condition whether there is a disturbance in the system. In this case, the optimization algorithm needs to wait for the next SS condition to run the cycle again. ROPA tackles this problem using dynamic data to update the model what avoids the steady-state wait issue. The application of these methodologies to the Propylene Chlorination process can show the benefits of using ROPA when compared to the classical RTO method, MPA. The results show that the ROPA is able to reach the stationary optimum even using transient data in a steady-state optimization. In this case study, ROPA and MPA results are similar since the system is a gas-phase process which has a fast dynamics. Because of this, the ROPA benefits cannot appear very different from MPA method. However, even with the fast dynamics issue, it can be seen that MPA deals with the steady-state wait what is the main drawback of the algorithm.

5.1 The process model

The second case study is the Propylene Chlorination process in which allyl chloride is produced. This is a commercial chemical used mainly as an intermediate in the manufacture of epichlorohydrin and glycerine (BOOZALIS et al., 1982). The considered process occurs in a gas-phase CSTR reactor with two feed streams as shown in Figure 16 below. In order to simulate a more realistic system, the process is simulated using the software Aspen Plus Dynamics.

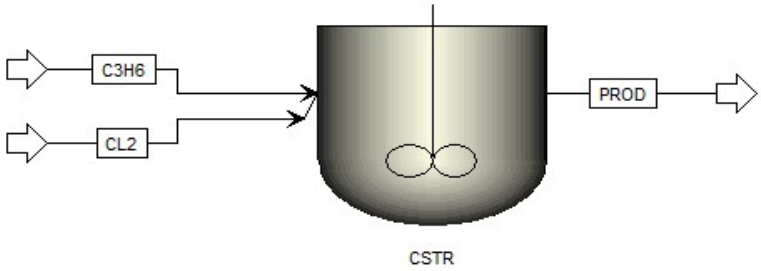

Figure 16 - Propylene Chlorination process simulated in Aspen Plus Dynamics (Source: own elaboration).

The process simulated in Aspen Plus Dynamics represents the real plant, and two feed streams are considered: Cl_2 and C_3H_6. The principal and desired product is the allyl chloride (C_3H_5Cl). The reactions in the process and the rate expressions for these reactions are based on Biegler and Hughes (1983). The first reaction (1) is substitution by chlorine to produce allyl chloride:

$$Cl_2 + C_3H_6 \overset{k1}{\rightarrow} C_3H_5Cl + HCl$$

The second reaction (2) is addition of chlorine that forms 1,2-dichloropropane:

$$Cl_2 + C_3H_6 \overset{k2}{\rightarrow} C_3H_6Cl_2$$

Finally, the third reaction (3) is chlorine substitution in allyl chloride to yield 1,3-dichloropropene:

$$Cl_2 + C_3H_5Cl \overset{k3}{\rightarrow} C_3H_4Cl_2 + HCl$$

All the three reactions are exothermic and have overall second-order Arrhenius-type kinetics. The rate expressions and kinetic constants are considered as follows:

$$r_j = k_j p_j{}^* p_{Cl_2} \quad (31)$$

where

$$k_j = A_j e^{\left[\frac{-B_j}{T_R}\right]} \quad (32)$$

in which $j = 1,2,3$ is related to the reactions 1, 2 and 3, respectively. p_{j^*} is the partial pressure of propylene for reactions 1 and 2 and of allyl chloride for reaction 3. The constants A_j and B_j are given in Table 2.

In order to simplify the model, the gas is assumed to be ideal. Thus, the rate expressions (31) can be replaced by (34) considering the equation of state of an ideal gas, as shown below:

$$P_i V = N_i RT \tag{33}$$

and

$$r_j = k_j N_{j^*} N_{Cl_2} \left(\frac{RT}{V}\right)^2 \tag{34}$$

After the rate expressions are established, the material balance for all of the species in the system is given by (35).

$$\begin{aligned}
\frac{dN_{HCl}}{dt} &= -F_{out_{HCl}} + (r_1 + r_3)V \\
\frac{dN_{Cl_2}}{dt} &= F_{in_{Cl_2}} - F_{out_{Cl_2}} + (-r_1 - r_2 - r_3)V \\
\frac{dN_{C_3H_6}}{dt} &= F_{in_{C_3H_6}} - F_{out_{C_3H_6}} + (-r_1 - r_2)V \\
\frac{dN_{C_3H_5Cl}}{dt} &= -F_{out_{C_3H_5Cl}} + (r_1 - r_3)V \\
\frac{dN_{C_3H_6Cl_2}}{dt} &= -F_{out_{C_3H_6Cl_2}} + (r_2)V \\
\frac{dN_{C_3H_4Cl_2}}{dt} &= -F_{out_{C_3H_4Cl_2}} + (r_3)V
\end{aligned} \tag{35}$$

where F_{in} and F_{out} are the inlet and outlet molar flow rate and r_1, r_2 and r_3 are the corresponding rate expressions.

As the number of moles is changing and the pressure in the reactor is constant, it is necessary to consider that F_{out} changes during the process. F_{out} is calculated as shown below:

$$\sum_{i=1}^{N_c} \frac{dN_i}{dt} = F_{in} - F_{out} + \left(\sum_{i=1}^{N_c} \sum_{j=1}^{N_r} \alpha_{ij} r_j\right) V \quad (36)$$

where

$$\sum_{i=1}^{N_c} N_i = \frac{PV}{RT} \quad (37)$$

and

$$\sum_{i=1}^{N_c} \frac{dN_i}{dt} = -\frac{PV}{RT^2} \frac{dT}{dt} \quad (38)$$

where N_c and N_r are the number of components and the number of reactions, respectively. Substituting (38) into (36) and considering the stoichiometry of the reactions, the output flow rate is given by (39).

$$F_{out} = F_{in} - k_2 N_{C_3H_6} N_{Cl_2} \left(\frac{RT}{V}\right)^2 V + \frac{PV}{RT^2} \frac{dT}{dt} \quad (39)$$

Regarding the energy balance, the kinetic energy terms and the energy needed for mixing the reactor are neglected to simplify the energy balance. The energy balance is given by the following equations, and it is based on Mäkilä and Waller (1980).

$$\frac{dU}{dt} = \dot{H}_f - \dot{H} - \dot{Q} \quad (40)$$

where U is the internal energy, $\dot{H}$ is the flow of enthalpy, and $\dot{Q}$ denotes the heat flow from the reactor. As the volume of the reactor is considered constant, the energy balance takes the form below:

$$\frac{dH}{dt} - V \frac{dp}{dt} = \dot{H}_f - \dot{H} - \dot{Q} \quad (41)$$

Assuming the following thermodynamics relations (42) - (45), the energy balance is given by (46), as shown below:

$$dH - Vdp = C_p dT - \left[\left(\frac{\partial H}{\partial p}\right)_{T,N} - V\right] dp + h^T dN \tag{42}$$

$$-T\left(\frac{\partial V}{\partial T}\right)_{p,N} = \left(\frac{\partial H}{\partial p}\right)_{T,N} - V \tag{43}$$

$$-\left[\left(\frac{\partial H}{\partial p}\right)_{T,N} - V\right]\left(\frac{\partial p}{\partial T}\right)_{V,N} = C_p - C_v \tag{44}$$

$$dp = \left(\frac{\partial p}{\partial T}\right)_{V,N} dT + \left[\left(\frac{\partial p}{\partial N}\right)_{T,V}\right]^T dN \tag{45}$$

$$C_v \frac{dT}{dt} + \left[-T\left(\frac{\partial V}{\partial T}\right)_{p,N}\left[\left(\frac{\partial p}{\partial N}\right)_{T,V}\right]^T + h^T\right]\frac{dN}{dt} = \dot{H}_f - \dot{H} - \dot{Q} \tag{46}$$

Considering that $N = CV$ in the material balance in which C is the vector of the molar concentrations of the species at time t, the energy balance can be written as (47).

$$C_v \frac{dT}{dt} + \left[-T\left(\frac{\partial V}{\partial T}\right)_{p,N}\left[\left(\frac{\partial p}{\partial N}\right)_{T,V}\right]^T + h^T\right]\frac{dN}{dt} = \left({h_f}^T - h^T\right)C_f \dot{V}_f - \Delta h^T r V - \dot{Q} \tag{47}$$

where Δh is the vector of the heats of the reactions.

The energy balance can be simplified in the following way in order to assume an ideal mixture of gases in the reactor. The equation of state for an ideal gas is given by (48):

$$pV = \sum_i N_i RT \tag{48}$$

gives

$$-T\left(\frac{\partial V}{\partial T}\right)_{p,N} = -V \tag{49}$$

as well as

$$\left(\frac{\partial p}{\partial N_i}\right)_{T,V} = \frac{RT}{V} \tag{50}$$

thus:

$$\left(\frac{\partial p}{\partial N}\right)_{T,V}{}^{T} \frac{dN}{dt} = RT\frac{dC_{tot}}{dt} \tag{51}$$

where C_{tot} is the vector of total molar concentration of the species.

Moreover, the partial enthalpies are given by (52):

$$h = \int_{T_R}^{T} C_p dT + h_R \tag{52}$$

where T_R is a reference temperature and h_R is the corresponding partial molar enthalpies.

Substituting these equations into the energy balance (47), the energy balance for the case study can be:

$$C_v \frac{dT}{dt} = \left[\int_{T}^{T_f} {C_p}^{T} dT\right] C_{in}\dot{V}_{in} - \Delta h^{T} rV - \dot{Q} + RT\frac{dN_{tot}}{dt} \tag{53}$$

The process condition and the nominal values of the parameters are listed in Table 2.

Table 2 - Process condition and parameter set of the Propylene Chlorination model. The values are based on Biegler and Hughes (1983). The lower and upper bounds of the manipulated variables and the parameters are used in the economic optimization layer in the ROPA and MPA cycles.

	Variable(symbol) [unit]	Lower bound	Nominal Value	Upper bound
-	Reactor volume (V) $[\mathrm{ft}^3]$	-	100	-
-	Reactor pressure (P) $[\mathrm{atm}]$	-	72.28	-
-	Heat capacity (C_p) $[\mathrm{BTU/lbmol\ °R}]$	-	35	-
-	Heat of reaction 1 (Δh_1) $[\mathrm{BTU/lbmol}]$	-	-4800	-
-	Heat of reaction 2 (Δh_2) $[\mathrm{BTU/lbmol}]$	-	-79200	-
-	Heat of reaction 3 (Δh_3) $[\mathrm{BTU/lbmol}]$	-	-91800	-
-	Gas constant (R) $[\mathrm{BTU/lbmol\ °R}]$	-	1.987	-
-	Flow of reactant Cl_2 $(F_{in_{Cl_2}})$[lbmol/h]	-	25.3532	-
$\boldsymbol{u_1}$	Flow of reactant C_3H_6 $(F_{in\ _{C_3H_6}})$[lbmol/h]	800	101.4128	1050
$\boldsymbol{u_2}$	Reactor inlet temperature (T_{in})[ºR]	1000	1300	1400
$\boldsymbol{x_1}$	Number of moles of HCl (N_{HCl})[lbmol]	-	0.1976440	-
$\boldsymbol{x_2}$	Number of moles of Cl_2 (N_{Cl_2})[lbmol]	-	0.0001488	-
$\boldsymbol{x_3}$	Number of moles of C_3H_6 $(N_{C_3H_6})$[lbmol]	-	0.6885350	-
$\boldsymbol{x_4}$	Number of moles of C_3H_5Cl $(N_{C_3H_5Cl})$[lbmol]	-	0.0241817	-
$\boldsymbol{x_5}$	Number of moles of $C_3H_6Cl_2$ $(N_{C_3H_6Cl_2})$[lbmol]	-	0.0027597	-
$\boldsymbol{x_6}$	Number of moles of $C_3H_4Cl_2$ $(N_{C_3H_4Cl_2})$[lbmol]	-	0.0867309	-
$\boldsymbol{x_7}$	Reactor temperature (T)[ºR]	-	1000	-
$\boldsymbol{p_1}$	A_1[lbmol/h ft³ atm²]	-	206000	-
$\boldsymbol{p_2}$	B_1[ºR]	-	13600	-
$\boldsymbol{p_3}$	A_2[lbmol/h ft³ atm²]	-	11.7	-
$\boldsymbol{p_4}$	B_2[ºR]	-	3430	-
$\boldsymbol{p_5}$	A_3[lbmol/h ft³ atm²]	-	$4.6e^8$	-
$\boldsymbol{p_6}$	B_3[ºR]	-	21300	-

It is important to note that since the process dynamic is significantly fast, it is not desirable in a ROPA implementation which aims at comparing ROPA to the MPA method. In order to decrease the process dynamic, it is considered that the reactor is thickly covered in steel with a mass of 10000 lb.

5.2 Economic Optimization

The economic optimization aims at optimizing the process economically. The objective function is the unit profit, Φ_{profit}, and the objective is to maximize this function. The optimization problem is based on Biegler and Hughes (1983), and it can be described as in (54).

$$\Phi_{profit} = 22.17(AC) + 12.48(DPC) + 10.06(DCP^*) \quad (54)$$

where AC, DPC and DCP^* are the product rates for allyl chloride (C_3H_5Cl), dichloropropane ($C_3H_6Cl_2$) and dichloropropene (C_3H_4Cl), respectively. All the rates are in lbmol/h, and the profit has units of $/h.

In the RTO cycle, the economic optimization is a constrained optimization problem where the set of constraints is composed of the model equations and operational inequality constraints. For ROPA and MPA, the model equations represent the plant in steady-state condition, and the operational inequality constraints are the lower and upper bounds as shown in Table 2.

5.3 Process Simulation

The process simulations are performed using MATLAB, Aspen Plus Dynamics and Sundials (HINDMARSH et al., 2005). In order to simulate a more realistic process, the system is simulated in Aspen Plus Dynamics in which transient data are collected as the plant measurements, $y_{p,k}$. Sundials is used to provide the sensitivities equations that are used in the online estimation step, in the Extended Kalman filter equations. MATLAB runs the real-time optimization using all of the given information.

The plant measurements, $y_{p,k}$, are the number of moles of the products C_3H_5Cl and $C_3H_6Cl_2$. A sensor is considered in order to measure these values in the outlet of the process, and random disturbances were admitted in the system to simulate a plant with noisy measurements, as shown in (55).

$$y_{n,k} = y_k + error \,.\, y_k \,.\, randn() \tag{55}$$

where $y_{n,k}$ is the measurement with noise at time k; y_k is its actual value; the $error$ is equal to 1%; and $randn$ draws a random scalar from the standard normal distribution.

The plant measurements are used in the RTO estimation layers to estimate the states and parameters in the current time. In the ROPA cycle, the parameters are estimated using the Extended Kalman filter (EKF) in which sensitivity equations are considered to obtain the matrixes which are used in the EKF algorithm. On the other hand, MPA estimates the parameters considering the model adaptation problem shown in (12). Both sets of estimated parameters for ROPA and MPA methods are used in the steady-state optimization problem obtaining the decision variables vector that is sent to the plant closing the RTO cycle, for this case study. A model predictive control (MPC) can be implemented in the RTO cycle; however, it is not mandatory. If an MPC layer is considered, the states estimated by the Extended Kalman filter are used as feedback values.

In the simulations, deterministic disturbances also affect the process. They are divided into measured and unmeasured disturbances. The measured disturbance affects the reactor inlet temperature (T_{in}), and the unmeasured disturbance changes the nominal values of the parameters. First, the model validation is done considering a step change of 400ºR in the inlet temperature value between the time interval of 3.75 and 12.75 hours and a step change in the nominal parameter values between 18.75 and 26.75 hours. For ROPA and MPA implementations, the step change of 400ºR in the inlet temperature value is added between 8 and 11.5 hours. Subsequently, the reaction parameters change their nominal values shown in Table 2 to [2.060, 13600, 0.00117, 3430, $4.6\mathrm{e}^3$, 21300].

The Extended Kalman filter is used to estimate the parameters and states in the ROPA cycle and to estimate the states in the MPA algorithm. Its tuning parameters are used in (21) - (24) and chosen as shown below in (56).

$$\begin{aligned} \boldsymbol{Q} &= diag([1e^{0};\ 1e^{0};\ 1e^{0};\ 1e^{0};\ 1e^{-2};\ 1e^{-2};\ 1e^{-6}]) \\ \boldsymbol{Q^p} &= diag([1e^{20};\ 0.4e^{-3};\ 8e^{2};\ 0.2e^{-3};\ 1e^{0};\ 0.5e^{-4}]) \\ \boldsymbol{R} &= diag([1e^{2};\ 1e^{2}]) \end{aligned} \tag{56}$$

where $\boldsymbol{Q}$, the covariance matrix of the process model, is related to the states ($N_{HCl}, N_{Cl_2}, N_{C_3H_6}, N_{C_3H_5Cl}, N_{C_3H_6Cl_2}, N_{C_3H_4Cl_2}, T$); $\boldsymbol{R}$, the measurement noise covariance matrix, is related to the measured variables ($N_{C_3H_5Cl}, N_{C_3H_6Cl_2}$); and $\boldsymbol{Q^p}$, the parameter covariance matrix, corresponds to the parameters ($A_1, B_1, A_2, B_2, A_3, B_3$). The values of $\boldsymbol{Q}$, $\boldsymbol{R}$ and $\boldsymbol{Q^p}$ are kept constants during the RTO implementations.

In the MPA method, the filter values for the steady-state detection step are tuned as shown below. Moreover, the critical value for the variance ratio, $\boldsymbol{R}_{crit}$, is also chosen for the case study. The weighting factor for the model adaptation algorithm, $\boldsymbol{R}_P$, is the identity matrix.

$\boldsymbol{\lambda}_1 = [0.2, 0.2]$, $\boldsymbol{\lambda}_2 = [0.1, 0.1]$, $\boldsymbol{\lambda}_3 = [0.1, 0.1]$, $\boldsymbol{R}_{crit} = [4.0, 7.0]$

where the first and second values of the arrays are related to the component C_3H_5Cl and $C_3H_6Cl_2$, respectively.

The stationary economic optimization was performed using the *fmincon* function in MATLAB for both of the RTO methods. The default algorithm for *fmincon*, the interior-point algorithm, was used in the optimization executions. The model summary for this process can be described as follows:

$$\begin{aligned}
\boldsymbol{x} &= [N_{HCl}, N_{Cl_2}, N_{C_3H_6}, N_{C_3H_5Cl}, N_{C_3H_6Cl_2}, N_{C_3H_4Cl_2}, T]^T \\
\boldsymbol{y} &= [N_{C_3H_5Cl}, N_{C_3H_6Cl_2}]^T \\
\boldsymbol{u} &= [F_{in\ C_3H_6}]^T \\
\boldsymbol{p} &= [p_1, p_2, p_3, p_4, p_5, p_6]^T = [A_1, B_1, A_2, B_2, A_3, B_3]^T
\end{aligned} \tag{57}$$

where $\boldsymbol{x}$ is the vector of the complete system model states, $\boldsymbol{y}$ is the vector of the measurements, $\boldsymbol{u}$ is the vector of the decision variable, and $\boldsymbol{p}$ is the vector of the adjustable parameters.

5.4 Results and discussion

The real plant is represented by the simulation performed in Aspen Plus Dynamics. The Propylene Chlorination process is simulated considering a gas-phase CSTR reactor. The process model validation is the first analysis in the considered RTO implementations. As it is known that the model must accurately represent the real process, the process model validation is an important task in the case study. The process simulation considers all disturbances and tuning parameters previously described in Section 5.3, and the plant data are collected in order to compare them to the model in MATLAB. Figure 17 and Figure 18 show the state profiles for the studied process considering a time horizon of 35 hours.

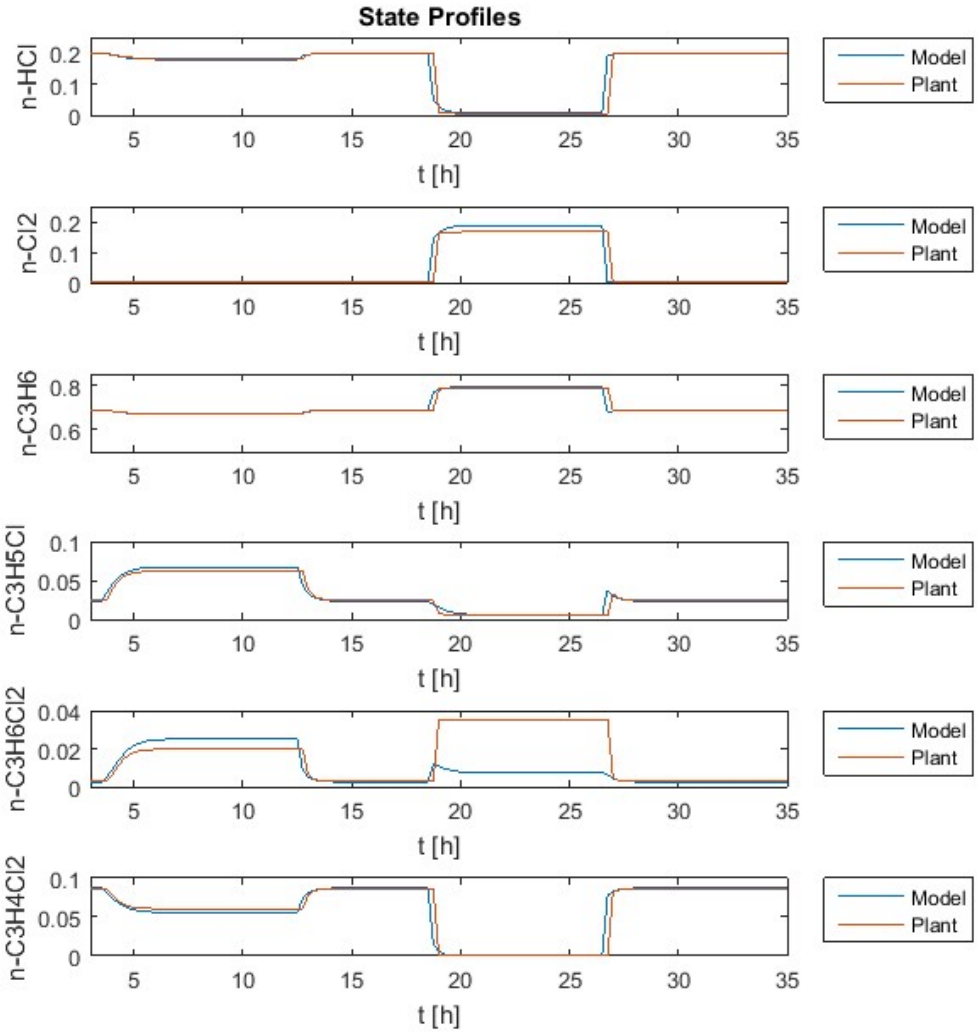

Figure 17 - Propylene Chlorination process model validation. The number of moles of each component in the process is in lbmol (Source: own elaboration).

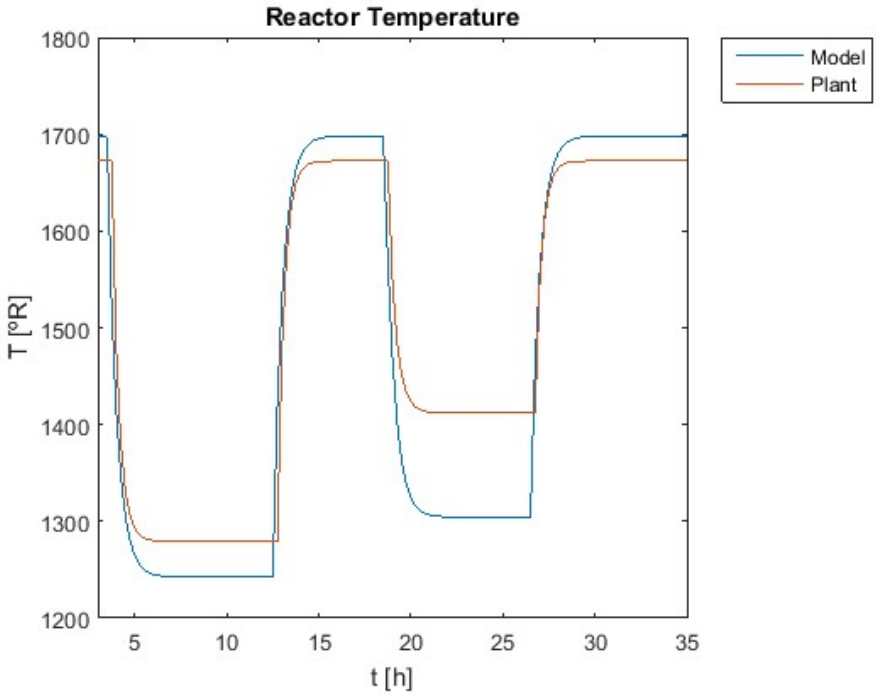

Figure 18 - Propylene Chlorination process model validation for the reactor temperature (Source: own elaboration).

The process model validation results show that the process dynamics can be properly represented by the proposed model. Although there is a bias between 18 and 27 hours in the fifth state profile shown in Figure 17, it is still considered that the model can satisfactorily represent the case study. This gap is due to the fact that there are differences between the Aspen Plus Dynamics model and the proposed model during the simulations.

The second analysis addresses the ROPA and MPA state estimation. Both of the RTO implementations use the Extended Kalman filter to estimate the states. Since the optimal decision predictions for ROPA and MPA are different, the state profiles are presented separately. Figure 19, Figure 20, Figure 21 and Figure 22 show the state estimation for ROPA and MPA. In the MPA cycle, only the states are estimated by the EKF while the states as well as the parameters are estimated by the EKF in the ROPA method. It can be seen that the estimated and actual state profiles are almost overlapped for both cases. It means that the filter uses a well tuned state covariance matrix, and it is working properly. As explained before, the estimated states could be used as feedback for the Model Predictive Control (MPC) implementation; however it is not done in the case study. If these state values are

properly predicted, the MPC performance is satisfactory since it is intrinsically connected with the estimation quality (MATIAS and LE ROUX, 2018).

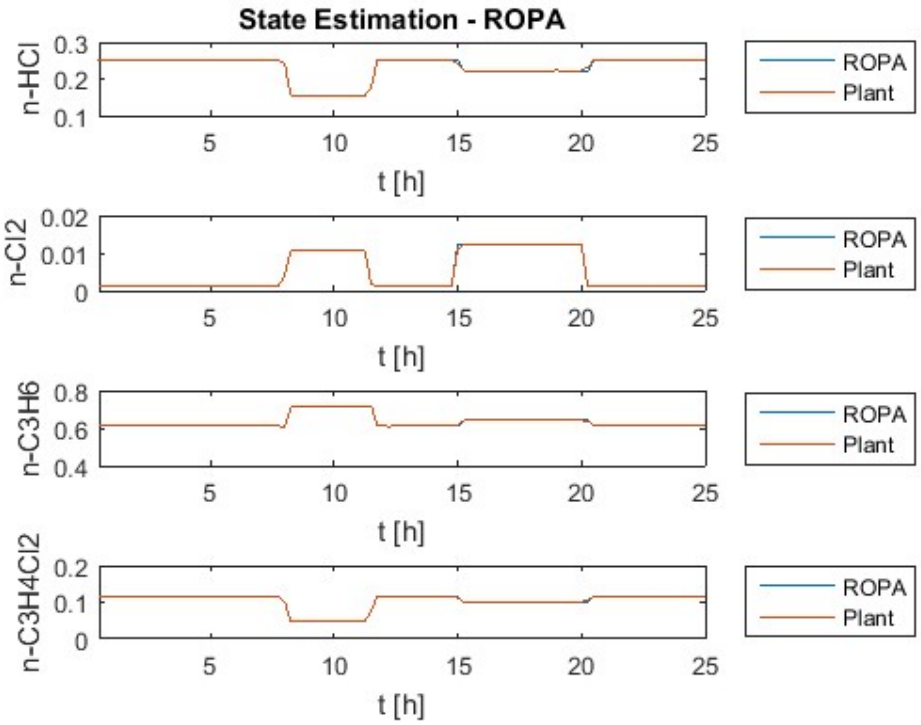

Figure 19 - State estimation for ROPA implementation in the Propylene Chlorination process using the Extended Kalman filter as the online estimator (Source: own elaboration).

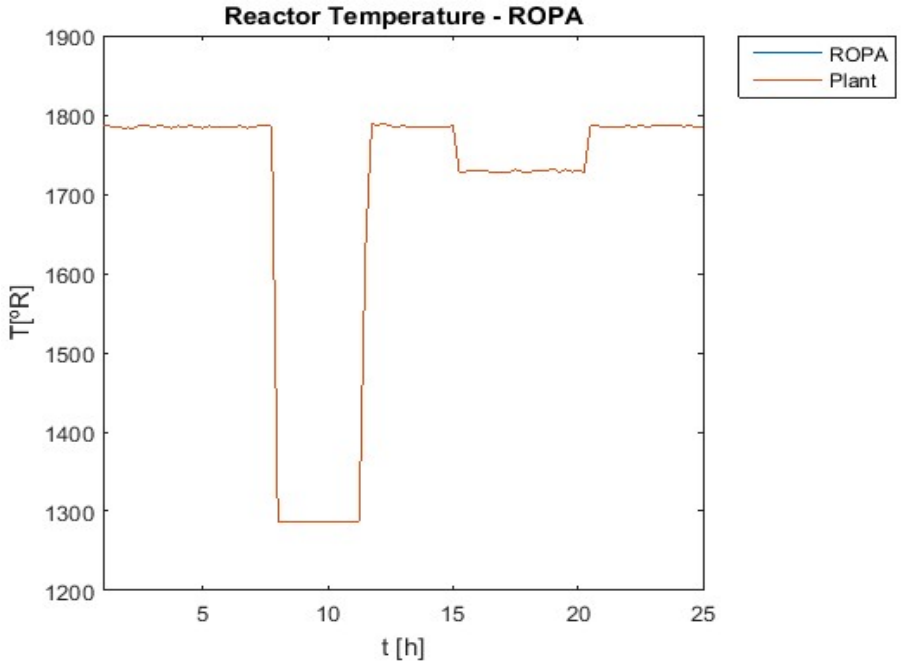

Figure 20 - Reactor temperature estimation for ROPA implementation in the Propylene Chlorination process using the Extended Kalman filter as the online estimator (Source: own elaboration).

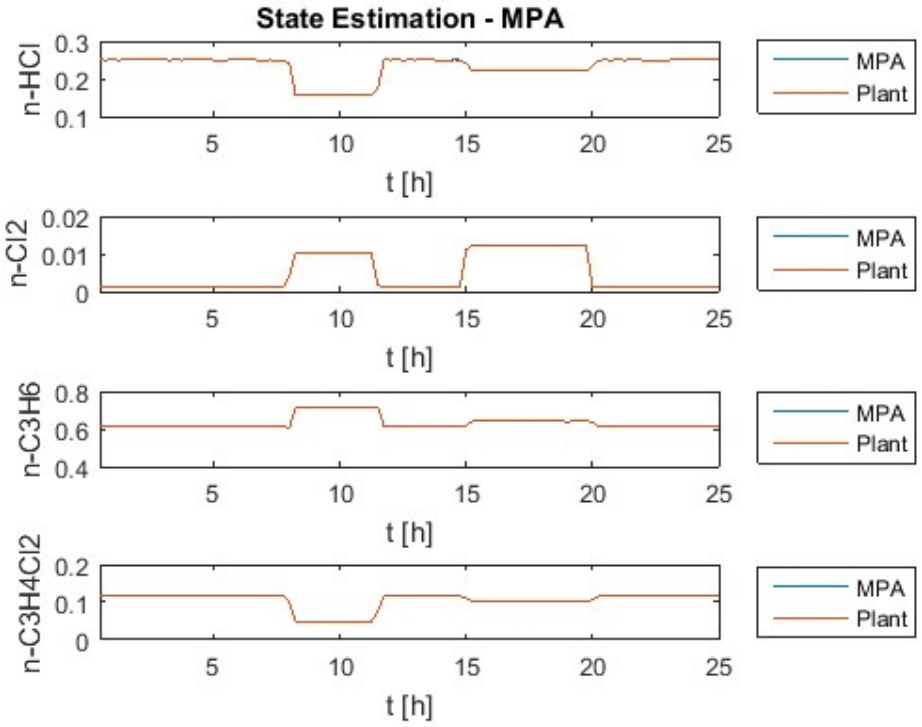

Figure 21 - State estimation for MPA implementation in the Propylene Chlorination process using the Extended Kalman filter as the online estimator (Source: own elaboration).

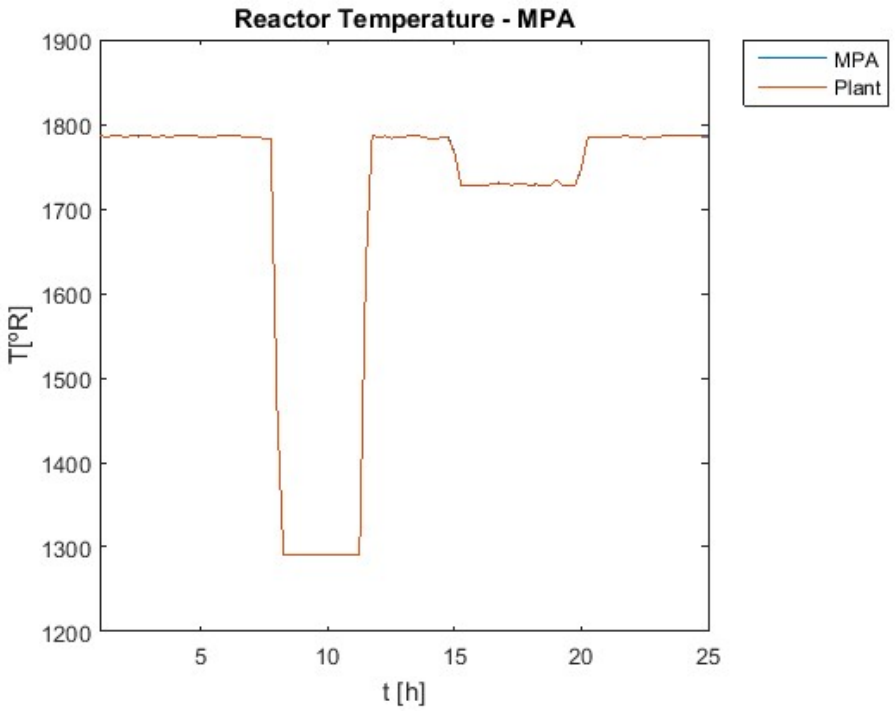

Figure 22 - Reactor temperature estimation for MPA implementation in the Propylene Chlorination process using the Extended Kalman filter as the online estimator (Source: own elaboration).

Regarding the parameter estimation, the MPA method uses the model adaptation problem shown in (12) while ROPA uses the Extended Kalman filter to estimate the adjustable parameters. The parameter disturbances that affect the system are the same for both of the methods, and the predicted parameter values are compared to the actual plant values as shown in Figure 23.

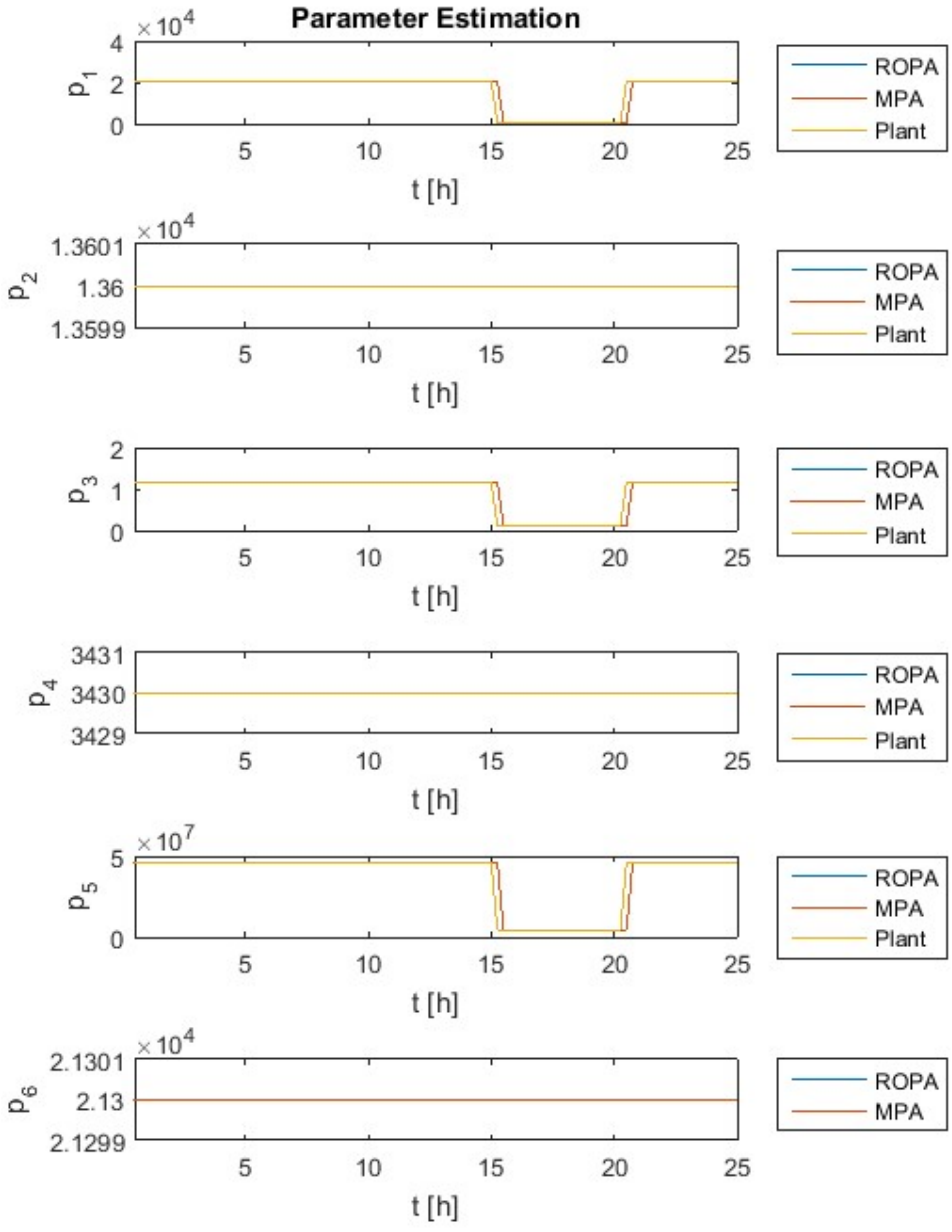

Figure 23 - Parameter estimation for ROPA and MPA implementations in the Propylene Chlorination process (Source: own elaboration).

As explained before, the parameter estimates for ROPA method are predicted by the EKF, and they are much closer to the actual nominal parameters (plant

values) than are those for the MPA implementation. This is due to the fact that if the system is perturbed, the ROPA method does not need to wait for the next steady-state condition to run the economic optimization cycle. On the other hand, the MPA method needs to detect the new SS point to optimize the process again what addresses the main disadvantage of the standard RTO method. It can be seen that after the disturbance in the nominal parameter values between 15 and 20 hours, the MPA method takes around 1 hour to reach the actual plant value while the ROPA methodology follows approximately the real value. As the EKF is used to estimate the parameter in the ROPA cycle, the results show that the parameter covariance matrix is well tuned for the case study.

In order to assess a more reliable performance result of both of the RTO implementations, it is important to address the economic and optimal decisions of the closed-loop optimization. Figure 24 and Figure 25 show the overall economic performance (the instantaneous profit) and the decision variables result, respectively.

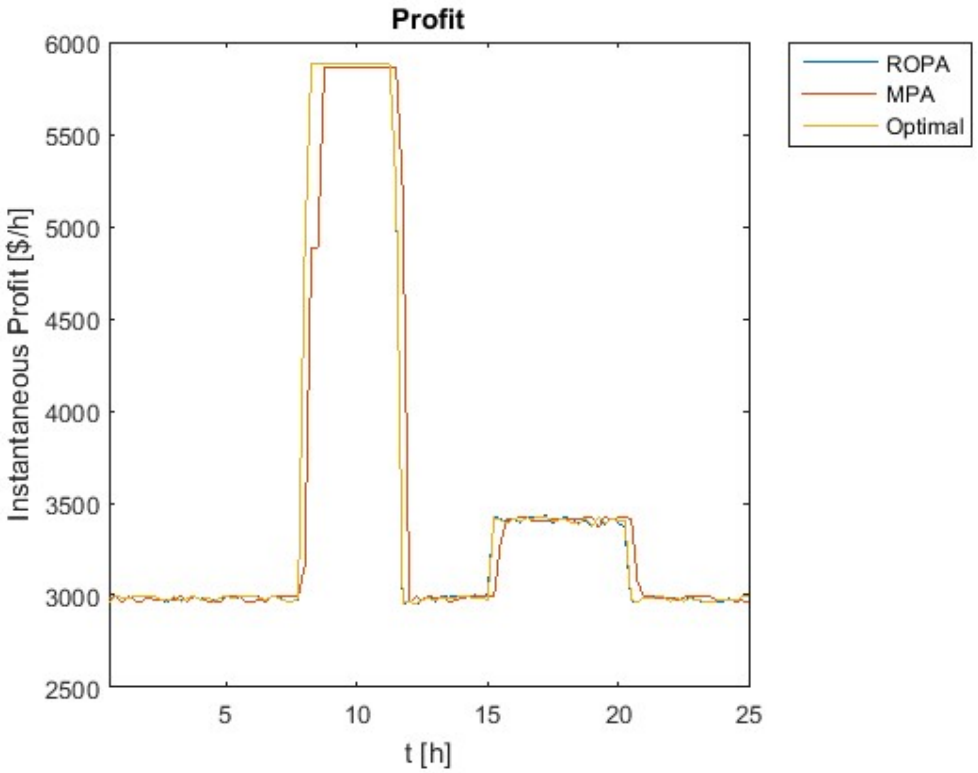

Figure 24 - Comparison between the instantaneous profit of the ROPA and MPA methods for the Propylene Chlorination process (Source: own elaboration).

According to the economic result shown in Figure 24, ROPA method can run the optimization cycle continually independently of any plant condition. Moreover,

ROPA is able to respond to both of the disturbances affecting the system. As MPA waits for the next steady-state value to optimize the process after a disturbance, the SS wait delay can again be seen in the economic result. Between 8 and 11.5 hours and 15 and 20 hours, there is a bias between the actual plant value and the value obtained by MPA. It is due to the SS detection step since the MPA estimates are updated only after the disturbances ceases what once more highlights the SS wait delay issue of the classical RTO method in the economic performance result.

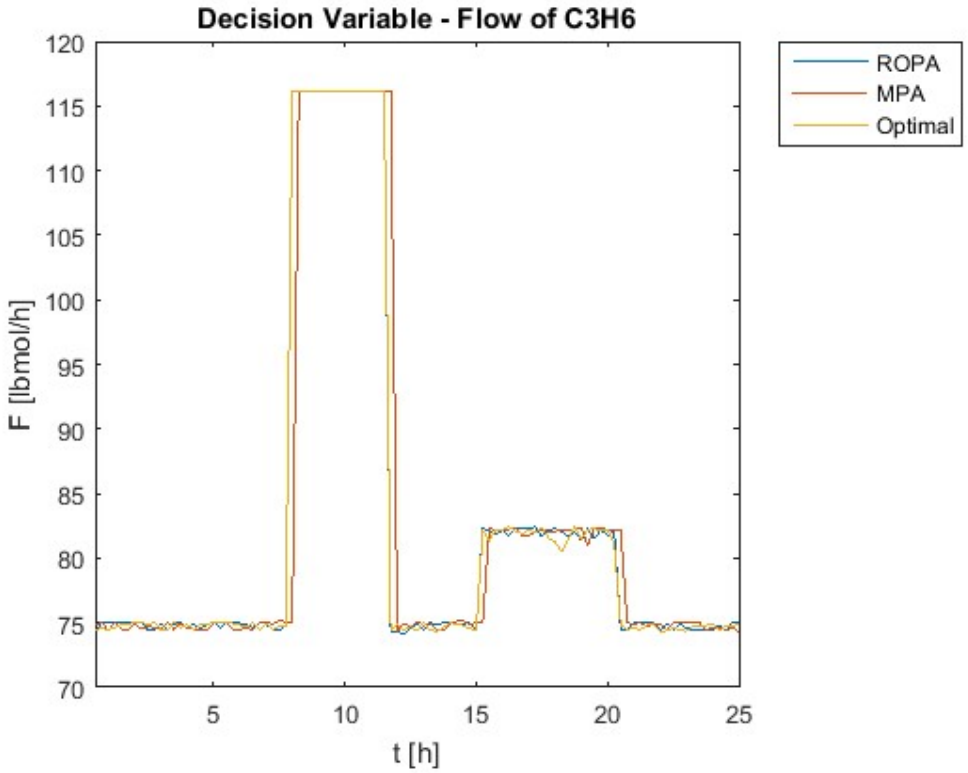

Figure 25 - Comparison between the plant optimal decision and the inputs calculated by ROPA and MPA implementations in the Propylene Chlorination process (Source: own elaboration).

The analysis of the decision variable in Figure 25 calculated by both of the methods can also show the ROPA benefits in the RTO cycle. The decision variable for the case study is the inlet molar flow rate of the reagent C_3H_6. The ROPA responses move towards the optimal plant value while the MPA results drift from the actual plant value during the RTO executions. As the parameter estimation in the MPA method is not reliable as in the ROPA, there is a considerable amount of parametric uncertainties. Since these unreliable parameter values are used to update the model in the SS optimization step, the plant is driven far from the optimality in the MPA implementation.

The application of the Real-time Optimization with Persistent Adaptation (ROPA) and the Model Parameter Adaptation (MPA) methods to the Propylene Chlorination process provides results that emphasize the benefits of using online estimator in the RTO cycle. ROPA uses transient data to update the model that is used in the stationary optimization layer while MPA uses only steady-state points. The main advantage of ROPA is that the detection of the SS condition is not necessary avoiding the SS wait delay issue. Thus, the frequency of the predictions and optimization executions enhances when compared to the MPA, hence ROPA can continually predict the states/parameters and optimize the plant in any plant condition, even under disturbances. The steady-state wait is not an issue when an online estimator is used to predict the parameters in the optimization cycle.

In the case study of the Propylene Chlorination process, it can be seen that the MPA and ROPA responses are similar. It is due to the fact that the process is a gas-phase system, and its dynamics is fast. The ROPA benefits can be seen better when the method is applied in a process with a slow dynamics in which after a disturbance, the system takes a significant time to reach the next steady-state operation point emphasizing the greatest advantage of ROPA implementation. When the dynamics is slow, the difference between MPA and ROPA is greater and more notable. Otherwise, the RTO implementations results are not very different from each other as in the studied process.

5.5 Conclusions

The Propylene Chlorination process is used as the representation of a plant in which two RTO methodologies are implemented: the Real-time Optimization with Persistent Adaptation (ROPA) and the Model Parameter Adaptation (MPA). The main goal of this application is to compare both of the methods showing the benefits of using the online estimation in the RTO cycle. In the ROPA implementation, transient data are used to estimate the parameters which are used in the stationary optimization step. On the other hand, MPA starts the optimization cycle with the detection of the steady-state condition and estimates the parameter values by the model adaptation problem obtaining the adjustable parameters that are used in the SS optimization layer. Thus, if the process is affected by a disturbance, MPA cannot run the RTO cycle until the system reaches the new SS condition promoting a delay

in the method's responses. ROPA runs the economic optimization independently of the plant condition what decreases the period between two sequential optimization executions since it avoids the steady-state wait.

The main contribution of this case study is the application of a new RTO method (ROPA) which does not change significantly the formulation of the standard RTO method (MPA) aiming at exposing the benefits of using this framework. Moreover, the simulation of the plant in the software Aspen Plus Dynamics, a commercial dynamic simulator, provides the use of a more realistic RTO implementation, being optimized by an external MPA and ROPA algorithm in MATLAB. The use of dynamic data to update the model during the optimization runs brings a great advantage. Generally, the detection of the steady-state condition is a problematic task in real processes in industries. It is because even meeting the methods' criteria that analyze if the process has reached the SS point, it can be hard to assure the process is really at steady-state. The results of the considered case study show that the integration of an online estimator can tackle the SS wait issue in the RTO cycle.

As explained before, ROPA avoids the steady-state detection due to the use of transient information. Hence, ROPA is able to run the optimization cycle even under disturbances what is the main benefit of the method. These dynamic measurements are used to estimate the parameters by an online estimator. The target of the ROPA is to continuously improve the RTO response obtaining the setpoints which reach the stationary plant optimum in the current time. Furthermore, ROPA is a hybrid RTO method that is between the dynamic and static RTO methodologies bringing advantage of decreasing the computational effort related to the dynamic RTO and avoiding the SS wait delay issue related to the static RTO, as explained before.

The application of ROPA to the Propylene Chlorination process brings results of the main benefits of using this methodology in the RTO executions. Moreover, applications of ROPA to more complex processes can handle with a plant-wide operation trying to tackle the standard RTO method's issues.

6 CONCLUDING REMARKS AND FUTURE WORK RECOMMENDATIONS

The Real-time Optimization with Persistent Adaptation (ROPA) method is applied to two different case studies in this thesis: (1) the Williams-Otto reactor; (2) the Propylene Chlorination process. ROPA is proposed by Matias and Le Roux (2018), and it is based on the idea of using dynamic data in the RTO cycle aiming at optimizing the plant economically. As the formulation of the standard RTO methodology does not change significantly in this new framework, ROPA is attractive for both the academia and the industry.

The main advantage of ROPA method is the use of transient information to update the model in the stationary optimization what eliminates the detection of the steady-state step tackling the SS wait issue related to the classical RTO method, the Model Parameter Adaptation (MPA). Even treating dynamic data in a SS optimization, the results of both applications show that ROPA can continuously improve the setpoints reaching the stationary plant optimum. In both of the case studies, the Model Parameter Adaptation method (MPA) is also applied to the processes in order to compare the RTO methods.

A future work that can be recommended is the use of Model Predictive Control (MPC) implementation in both the case studies. Considering that the steady-state optimization layer is followed by the MPC layer, the optimal setpoints found in the RTO cycle are sent to the controller which implements the decision variables in the plant. The complete system considering the RTO and MPC layers for ROPA and MPA methods is represented by Figure 4.

BIBLIOGRAPHY

ADETOLA, V.; GUAY, M. Integration of real-time optimization and model predictive control. *Journal of Process Control*, v. 20, p. 125-133, 2010.

AHMAD, A.; GAO, W.; ENGELL, S. A study of model adaptation in iterative real-time optimization of processes with uncertainties. *Computers and Chemical Engineering*, p. 1-10, 2018.

ASSIS, A. J. de; FILHO, R. M. Soft sensors development for on-line bioreactor state estimation. *Computers and Chemical Engineering*, v. 24, p. 1099-1103, 2000.

BAZARAA, M. S.; SHERALI, H. D.; SHETTY, C. M. Nonlinear Programming: Theory and Algorithms: 3. ed. New Jersey: WILEY INTERSCIENCE, 2006.

BIEGLER, L. T.; HUGHES, R. R. Process Optimization: A Comparative Case Study. *Computers and Chemical Engineering*, v. 7, p. 645-661, 1983.

BHAT, S. A.; SARAF, D. N. Steady-state identification, gross error detection, and data reconciliation for industrial process units. *Industrial and Engineering Chemistry Research*, v. 43, p. 4323-4336, 2004.

BOOZALIS, T. S.; IVY, J. B.; WILLIS, G. G. *Allyl chloride process*, US4319062A, 1982.

CAO, S.; RHINEHART, R. R. An efficient method for on-line identification of steady-state. *Journal of Process Control*, v. 5, p. 363–374, 1995.

CAO, S.; RHINEHART, R. R. Critical values for a steady-state identifier. *Journal of Process Control*, v. 7, n.2 p. 149–152, 1997.

CUTLER, C. R.; PERRY, R. T. Real time optimization with multivariable control is required to maximize profits. *Computers and Chemical Engineering*, v. 7, n. 5, p. 663-667, 1983.

DARBY, M. L.; NIKOLAOU, M.; JONES, J.; NICHOLSON, D. RTO: An overview and assessment of current practice. *Journal of Process Control*, v. 21, p. 874-884, 2011.

DIEHL, M.; BOCK, H. G.; SCHLÖDER, J. P.; FINDEISEN, R.; NAGY, Z.; ALLGÖWER, F. Real-time optimization and nonlinear model predictive control of processes governed by differential-algebraic equations. *Journal of Process Control*, v. 12, p. 577–585, 2002.

ENGELL, S. Feedback control for optimal process operation. *Journal of Process Control*, v. 17, p. 203-219, 2007.

FRIEDMAN, Y. Z. What's wrong with unit closed loop optimization. *Hydrocarbon Processing*, 1995.

GRACIANO, J. E. A. *Real-time Optimization in chemical processes: evaluation of strategies, improvements and industrial application.* Doctoral dissertation. University of Sao Paulo, Sao Paulo, 2015.

GROSSMANN, I. E.; BIEGLER, L. T. Optimizing chemical processes. *American Chemical Society*, 1995.

HINDMARSH, A. E.; BROWN, P. N.; GRANT,K. E.; LEE, S. L.; SERBAN, R.; SHUMAKER, D. E. WOODWARD, C. S. SUNDIALS: Suite of nonlinear and differential/algebraic equation solvers. *ACM Transactions on Mathematical Software (TOMS)*, 2005.

JIA, M.; CHEN, C.; KOU, W.; NIU, D.; WANG, F. Real-time optimization of converter inlet temperature in acid production with flue gas. *Chemical Engineering Research and Design*, v. 122, p. 226-232, 2017.

JIANG, T.; CHEN, B.; HE, X.; STUART, P. Application of steady-state detection method based on wavelet transform. *Computers and Chemical Engineering*, v. 27, p. 569-578, 2003.

KRISHNAMOORTHYA, D.; FOSS, B.; SKOGESTAD, S. Steady-state real-time optimization using transient measurements. *Computers and Chemical Engineering*, v. 115, p. 34-35, 2018.

M, G.; P, A. K.; JEROME, J. Comparative Assessment of a Chemical Reactor using Extended Kalman Filter and Unscented Kalman Filter. *Procedia Technology*, v. 14, p. 75 – 84, 2014.

MÄKILÄ, P. M.; WALLER, K. V. The Energy Balance in Modeling Gas-Phase Chemical Reactor Dynamics. *Chemical Engineering Science*, v. 36, p. 643–652, 1981.

MATIAS, J. O. A. Real-time optimization with persistent parameter adaptation using online parameter estimation. Doctoral dissertation. University of Sao Paulo, Sao Paulo, 2018.

MATIAS, J. O. A.; LE ROUX, G. A. C. Real-time optimization with persistent parameter adaptation using online parameter estimation. *Journal of Process Control*, v. 68, p. 195-204, 2018.

MENDOZA, D. F.; PALACIO, L. M.; GRACIANO, J. E. A.; RIASCOS, C. A. M.; VIANNA JR, A. S.; ROUX, G. A. C. L. Real-time optimization of an industrial-scale vapor recompression distillation process. Model validation and analysis. *Industrial & Engineering Chemistry Research*, v. 52, p. 5735-5746, 2013.

PAPASAVVAS, A.; FERREIRA, T. de A.; MARCHETTI, A. G.; BONVIN, D. Analysis of output modifier adaptation for real-time optimization. *Computers and Chemical Engineering*, v. 121, p. 285-293, 2019.

PRAKASH, J.; HUANG, B.; SHAH, S. L. Recursive constrained state estimation using modified extended Kalman filter. *Computers and Chemical Engineering*, v. 65, p. 9–17, 2014.

QUELHAS, A. D.; JESUS, N. J. C. de; PINTO, J. C. Common vulnerabilities of RTO implementations in real chemical processes. *Canadian Journal of Chemical Engineering*, v. 91, n. 4, p. 652-668, 2013.

RINCÓN, F. D.; LE ROUX, G. A. C.; LIMA, F. V. A novel ARX-based approach for the steady-state identification analysis of industrial depropanizer column datasets. *Processes*, v. 3, n. 2, p. 257-285, 2015.

SCHLADT, M.; HU, B. Soft sensors based on nonlinear steady-state data reconciliation in the process industry. *Chemical Engineering and Processing*, v. 46, p. 1107–1115, 2007.

SMITH, J. M. Chemical Engineering Kinetics, 2nd Edn. McGraw-Hill, New York (1970).

ZANIN, A. Implementação industrial de um otimizador em tempo real. Doctoral dissertation. University of Sao Paulo, Sao Paulo, 2001.